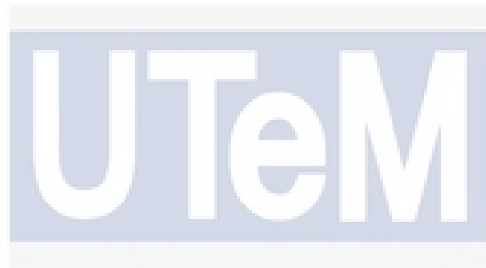


**INVESTIGATION ON TiO_2 /GRAPHENE SCHOTTKY JUNCTION
FOR VOLATILE ORGANIC COMPOUND GASES**

MUHAMMAD HAZIQ BIN NOR AZMI



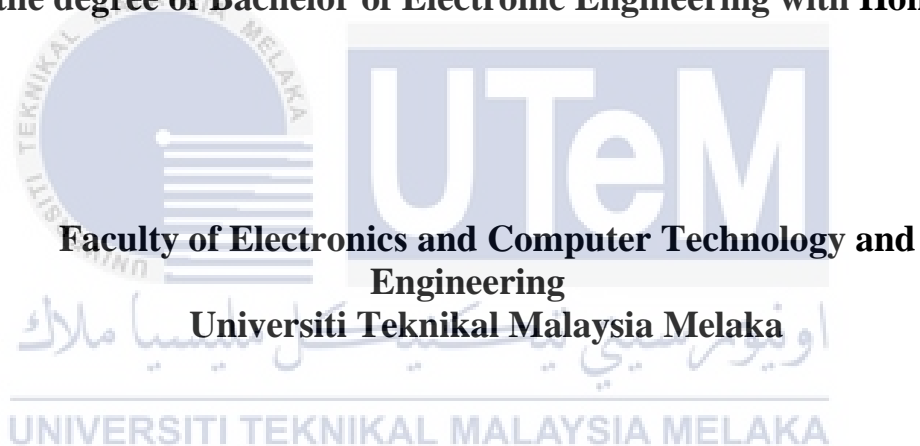
اونيورسيتي تيكنيكل مليسيا ملاك

UNIVERSITI TEKNIKAL MALAYSIA MELAKA
UNIVERSITI TEKNIKAL MALAYSIA MELAKA

**INVESTIGATION ON TiO_2 /GRAPHENE SCHOTTKY
JUNCTION FOR VOLATILE ORGANIC COMPOUND GASES**

MUHAMMAD HAZIQ BIN NOR AZMI

**This report is submitted in partial fulfilment of the requirements
for the degree of Bachelor of Electronic Engineering with Honours**



2024

BORANG PENGESAHAN STATUS LAPORAN
PROJEK SARJANA MUDA II

Tajuk Projek : Investigation on TiO₂/Graphene Schottky junction
for volatile organic compound gases
Sesi Pengajian : 2023/2024

Saya MUHAMMAD HAZIQ BIN NOR AZMI mengaku membenarkan laporan
Projek Sarjana Muda ini disimpan di Perpustakaan dengan syarat-syarat
kegunaan seperti berikut:

1. Laporan adalah hakmilik Universiti Teknikal Malaysia Melaka.
2. Perpustakaan dibenarkan membuat salinan untuk tujuan pengajian sahaja.
3. Perpustakaan dibenarkan membuat salinan laporan ini sebagai bahan
pertukaran antara institusi pengajian tinggi.²
4. Sila tandakan (✓):



SULIT*

(Mengandungi maklumat yang berdarjah
keselamatan atau kepentingan Malaysia
seperti yang termaktub di dalam AKTA
RAHSIA RASMI 1972)



TERHAD*

(Mengandungi maklumat terhad yang
telah ditentukan oleh organisasi/badan di
mana penyelidikan dijalankan.



TIDAK TERHAD

Disahkan oleh:



(TANDATANGAN PENULIS)



(COP DAN TANDATANGAN PENYELIA)

Alamat Tetap: No.2, Jalan
Suakasih 3/1F, Bandar Tun
Hussein Onn, 43200, Cheras,
Selangor

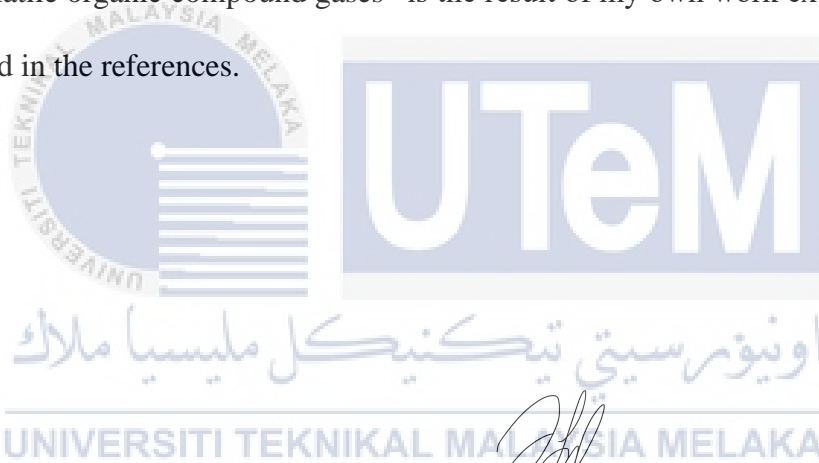
TS. DR. SITI AMANAH BINTI MOHD CHACHULI
Pensyarah Kanan
Fakulti Teknologi dan Kejuruteraan Elektronik dan Komputer
Universiti Teknikal Malaysia Melaka

Tarikh : 12 January 2024

Tarikh : 12 January 2024

DECLARATION

I declare that this report entitled “Investigation on TiO₂/Graphene Schottky junction for volatile organic compound gases” is the result of my own work except for quotes as cited in the references.



Signature :

Author : Muhammad Haziq Bin Nor Azmi

Date : 12 January 2024

APPROVAL

I hereby declare that I have read this thesis and in my opinion this thesis is sufficient in terms of scope and quality for the award of Bachelor of Electronic Engineering with Honours.



اونيورسيتي تكنولوجيكيك ماليسيا ملاك

Sarah

Signature :

UNIVERSITI TEKNIKAL MALAYSIA MELAKA

Supervisor Name : Ts. Dr. Siti Amaniah binti Mohd Chachuli

Date : 12 January 2024

ABSTRACT

A Schottky junction gas sensor is a junction formed between a metal and a semiconductor that forms a barrier, which can be modified by the presence of gas molecules. When gas molecules encounter the Schottky junction, they can change the properties of the semiconductor, such as its surface potential and charge carrier concentration. This, in turn, affects the electrical characteristics of the Schottky junction, such as its barrier height and capacitance. Due to the limitation of ohmic junction that has no diffusion barrier, external voltage can cause current to flow regardless of its polarity. To overcome this, Schottky junction is proposed in this project due to the formation of potential barrier at the interface. The goal of this project is to investigate the structure of Schottky junction gas sensor using Titanium dioxide/graphene ($\text{TiO}_2/\text{graphene}$) as sensing material for detecting volatile organic compound gases. This Schottky junction will be formed by attaching $\text{TiO}_2/\text{graphene}$ with silver that will be deposited using screen printing on a Kapton film substrate. Design 3 has higher response to acetone gas with the average value of 1.0255 compared to design 1 and 2 which has the average value of 1.0117 and 1.0222 respectively while design 2 has higher response to ethanol gas with the average value of 1.0586 compared to design 1 and 3 which has 1.0577 and 1.0339 respectively.

ABSTRAK

Sebuah sensor gas Schottky junction adalah suatu junction yang terbentuk antara logam dan semikonduktor yang membentuk suatu rintangan, yang boleh diubahsuai oleh kehadiran molekul gas. Apabila molekul gas berinteraksi dengan Schottky junction, mereka boleh mengubah sifat semikonduktor, seperti potensi permukaannya dan kepekatan pembawa cas. Ini pada gilirannya mempengaruhi ciri-ciri elektrik Schottky junction, seperti ketinggian rintangan dan kapasitans. Oleh kerana terdapat kekangan pada junction ohmik yang tidak mempunyai rintangan penyebaran, voltan luaran boleh menyebabkan arus mengalir tanpa mengira polaritinya. Untuk mengatasi ini, Schottky junction dicadangkan dalam projek ini kerana pembentukan rintangan potensial di antara muka. Tujuan projek ini adalah untuk menyelidiki struktur sensor gas Schottky junction menggunakan Titanium dioksida/grafin (TiO_2 /grafin) sebagai bahan pendeteksian untuk mengesan gas organik valatil. Schottky junction ini akan terbentuk dengan melekatkan TiO_2 /grafin dengan perak yang akan disadur menggunakan cetakan skrin pada substrat filem Kapton. Reka bentuk 3 menunjukkan tindak balas yang lebih tinggi terhadap gas aseton dengan nilai purata sebanyak 1.0255 berbanding dengan reka bentuk 1 dan 2 yang mempunyai nilai purata masing-masing sebanyak 1.0117 dan 1.0222.

ACKNOWLEDGEMENTS

I would like to express my deepest appreciation and gratitude to the individuals who have played a significant role in the completion of this thesis. Their unwavering support, guidance, and encouragement have been invaluable throughout this journey. First and foremost, I would like to thank Allah s.w.t for giving me this opportunity to pursue study and completing this thesis. I am also profoundly grateful to my supervisor Ts. Dr. Siti Amaniah Binti Mohd Chachuli for her exceptional guidance and expertise. Her insightful feedback, constructive criticism, and commitment to excellence have been instrumental in shaping this thesis. I am indebted to Universiti Teknikal Malaysia Melaka for providing the necessary resources and facilities that facilitated the development of this thesis. I would also like to acknowledge the support of my family and friends who have been a constant source of encouragement and motivation. Their unwavering belief in my abilities has been a driving force behind the completion of this thesis. Last but not least, I express my gratitude to all the researchers, scholars, and developers whose work has inspired and influenced the design of this thesis. In conclusion, I am thankful to everyone who has contributed to this project directly or indirectly. Your support has been invaluable, and I am truly appreciative of the collaborative spirit that has enriched the development of this thesis.

TABLE OF CONTENTS

| | |
|--|--------------|
| Declaration | |
| Approval | |
| Abstract | i |
| Abstrak | ii |
| Acknowledgements | iii |
| Table of Contents | iv |
| List of Figures | vii |
| List of Tables | ix |
| List of Symbols and Abbreviations | x |
| CHAPTER 1 INTRODUCTION | 1 |
| 1.1 Project Background | 1 |
| 1.2 Problem Statement | 2 |
| 1.3 Objectives | 3 |
| 1.4 Scope of Work | 3 |
| 1.5 Thesis Outline | 4 |
| CHAPTER 2 BACKGROUND STUDY | 6 |

| | | |
|------------------------------|---|-----------|
| 2.1 | General Overview | 6 |
| 2.2 | Previous Research on Schottky Junction Gas Sensor | 7 |
| 2.3 | Schottky Junction | 8 |
| 2.3.1 | Schottky Barrier Modulation | 9 |
| 2.4 | Sensing Material for VOC Gases | 9 |
| 2.4.1 | Tin (IV) Oxide (SnO_2) | 10 |
| 2.4.2 | Graphene | 11 |
| 2.4.3 | Titanium Dioxide (TiO_2) | 11 |
| 2.5 | Deposition Technique for Gas Sensor | 12 |
| 2.5.1 | Chemical Vapor Deposition | 13 |
| 2.5.2 | Hydrothermal | 14 |
| 2.5.3 | Screen Printing | 15 |
| 2.6 | Characteristics of Gas Sensor | 16 |
| 2.6.1 | Response | 17 |
| 2.6.2 | Sensitivity | 17 |
| 2.6.3 | Response Time and Recovery Time | 18 |
| CHAPTER 3 METHODOLOGY | | 20 |
| 3.1 | General Overview | 20 |
| 3.2 | Methodology Flowchart | 21 |
| 3.3 | Design Structure of Schottky Junction | 23 |

| | | |
|--|---|-----------|
| 3.4 | Preparation of Binder | 24 |
| 3.5 | Preparation of TiO ₂ /Graphene Paste | 25 |
| 3.6 | Fabrication of TiO ₂ /Graphene Schottky Junction | 28 |
| 3.6.1 | Electrode Deposition | 28 |
| 3.6.2 | Sensing Material Deposition | 28 |
| 3.7 | I-V Characteristics | 29 |
| 3.8 | Experimental Setup of Gas Sensor to Ethanol and Acetone | 30 |
| CHAPTER 4 RESULTS AND DISCUSSION | | 32 |
| 4.1 | General Overview | 32 |
| 4.2 | Fabrication of Gas Sensor | 33 |
| 4.3 | I-V Characteristics | 34 |
| 4.4 | Performance of Gas Sensor | 37 |
| 4.4.1 | Response to 25ml Acetone | 38 |
| 4.4.2 | Response to 25ml Ethanol | 40 |
| CHAPTER 5 CONCLUSION AND FUTURE WORKS | | 44 |
| 5.1 | Conclusion | 44 |
| 5.2 | Future Works | 45 |
| REFERENCES | | 47 |

LIST OF FIGURES

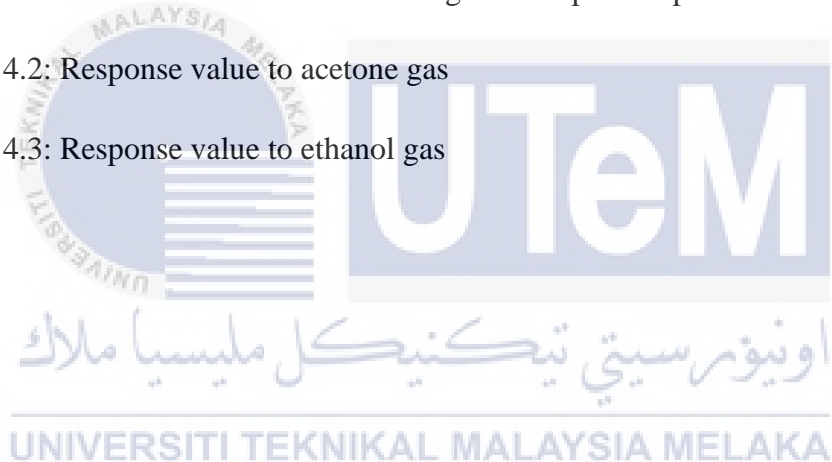
| | |
|---|----|
| Figure 2.1: Schematic diagram of Schottky barrier diode | 9 |
| Figure 2.2: SnO ₂ structure | 10 |
| Figure 2.3: Graphene structure | 11 |
| Figure 2.4: TiO ₂ structure | 12 |
| Figure 2.5: Chemical vapor deposition (CVD) technique | 14 |
| Figure 2.6: Hydrothermal technique | 15 |
| Figure 2.7: Screen printing technique | 16 |
| Figure 2.8: Response and recovery time using pulsed bias recovery (PBR) | 19 |
| Figure 3.1: Research methodology flowchart | 22 |
| Figure 3.2: 2D structure design of Schottky Junction in top view | 23 |
| Figure 3.3: Layout of Sensing Material | 24 |
| Figure 3.4: Layout of Electrode | 24 |
| Figure 3.5: Process of making binder | 25 |
| Figure 3.6: Preparation of TiO ₂ /graphene paste | 27 |
| Figure 3.7: Powder of each paste before adding binder | 27 |
| Figure 3.8: TiO ₂ /graphene paste | 27 |
| Figure 3.9: Electrode deposition | 28 |
| Figure 3.10: Sensing material deposition | 29 |

| | |
|--|----|
| Figure 3.11: I-V measurement of the gas sensor | 30 |
| Figure 3.12: Experimental setup of gas sensor measurement | 31 |
| Figure 4.1: Fabricated TiO ₂ /graphene (a) T99_G1_1, (b) T98_G2_1, (c) T95_G5_1, (d) T99_G1_2, (e) T98_G2_2, (f) T95_G5_2, (g) T99_G1_3, (h) T98_G2_3, and (i) T95_G5_3 | 23 |
| Figure 4.2: I-V characteristic (a) Design 1 (b) Design 2 (c) Design 3 | 35 |
| Figure 4.3: Response of TiO ₂ /graphene gas sensor to acetone vapor (a) Design 1 (b) Design 2 (c) Design 3 | 39 |
| Figure 4.4: Design 2 graph response to acetone gas | 42 |
| Figure 5.1: New design of Schottky junction structure (a) Layout of new structure of Schottky junction, (b) Sensing material layout, and (c) Electrode layout | 46 |



LIST OF TABLES

| | |
|---|----|
| Table 2.1: Characteristics of Schottky junction gas sensor | 7 |
| Table 3.1: Area (cm ²) of design | 24 |
| Table 3.2: Ratio for TiO ₂ /graphene paste | 25 |
| Table 4.1: Resistance value for each design of sample and paste | 37 |
| Table 4.2: Response value to acetone gas | 40 |
| Table 4.3: Response value to ethanol gas | 43 |



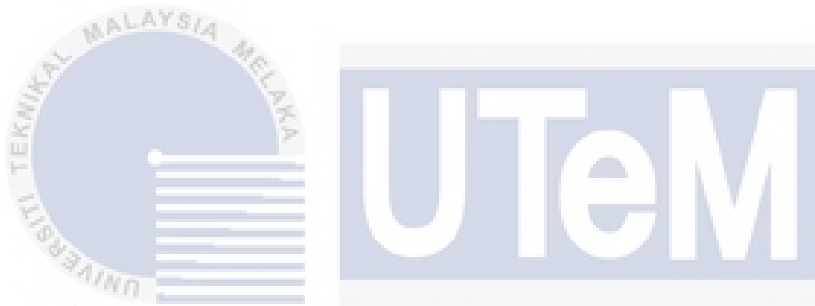
LIST OF SYMBOLS AND ABBREVIATIONS

| | | |
|------------------|---|---------------------------|
| TiO ₂ | : | Titanium Dioxide |
| VOC | : | Volatile Organic Compound |
| ppm | : | Part per million |
| CVD | : | Chemical Vapor Deposition |
| PBR | : | Pulsed Bias Recovery |
| rpm | : | Revolutions per minute |



CHAPTER 1

INTRODUCTION



1.1 Project Background

The project focuses on investigating the application of a TiO_2 /Graphene Schottky junction for detecting volatile organic compound (VOC) gases. Volatile organic compounds are organic chemicals that can easily evaporate into the air and are commonly found in products like paints, cleaning agents, fuels, and various industrial processes. These compounds can have adverse effects on human health and the environment, making their accurate and sensitive detection crucial.

The TiO_2 /Graphene Schottky junction is a promising candidate for gas sensing applications due to its unique properties. Titanium dioxide (TiO_2) is a wide-bandgap semiconductor known for its excellent chemical stability, high surface area, and ability to interact with various gases. Graphene, on the other hand, is a two-dimensional

carbon material with remarkable electrical, mechanical, and chemical properties. When combined, TiO₂ and graphene create a hybrid material with enhanced gas sensing capabilities.

The Schottky junction refers to a type of electronic interface formed between a semiconductor (TiO₂) and a metal (graphene), resulting in a rectifying behaviour due to the difference in work functions. This junction can efficiently facilitate charge separation and transport, which is essential for the gas sensing mechanism.

1.2 Problem Statement

Due to the limitation of the ohmic junction that has no diffusion barrier, application of external voltage causes current to flow regardless of its polarity. Schottky junction sensor may perform well compared to pristine material based ohmic sensor due to the formation of potential barrier at the interface [2]. The barrier height modulation of heterojunction sensor in presence of analyte environment causes incredible changes in the current flowing through the sensor [2]. Recently, it was demonstrated that Schottky contact could largely improve the sensitivity of gas sensors due to that Schottky barrier serves as a “gate” controlling the current passing through the barrier and the value of this current highly depends on the Schottky barrier height. Schottky junction-based gas sensors have been used widely because they have a low operating temperature, a high sensitivity, and a quick response time [2]. Because of the sensitive Schottky barrier height modulation by the surface chemisorbed gases and the amplification role played by the nanostructures to Schottky barrier effect, a high gas responsivity was achieved [1].

Volatile organic compound gases such as ethanol and acetone have been widely used in industrial production such as pharmaceuticals, cosmetics, and food. For acetone, it is a common colorless and transparent volatile organic compound and if human exposure is more than 450 mg/m³ (173 ppm), it can cause fatigue, headaches, and nervous system damage [7]. For ethanol, it is an important used in food, medical and health. However, prolonged exposure to high ethanol concentrations can easily result in uncomfortable symptoms such as skin irritation and reduce respiratory and neurological effects even with a concentration as low as 25 ppm [11]. Therefore, the creation of an acetone and ethanol detection device that is highly sensitive and can be used to detect ethanol or acetone leakage is crucial for both industrial safety and human health.



1.3 Objectives

To complete this investigation on TiO₂/Graphene Schottky junction for volatile organic compound gases, there are objectives that needs to be achieved which is:

- 1) To investigate the IV characteristics of Schottky junction gas sensor using TiO₂/graphene as sensing material.
- 2) To evaluate the TiO₂/graphene Schottky junction gas sensor to VOC gases at room operating temperature in terms of response.

1.4 Scope of Work

In this project, the goal is the investigation on TiO₂/Graphene Schottky junction for volatile organic compound gases. To further this investigation:

- 1) Titanium dioxide will be used as the main material while graphene is a dopant material that is chosen to be used as a sensing material for gas sensor.
- 2) Silver is chosen as an electrode for Schottky junction gas sensor.
- 3) Kapton film is chosen as a substrate.
- 4) Ethanol and acetone are chosen as volatile organic compound gases.
- 5) Screen printing technique is chosen as a deposition method for the electrode and sensing material.

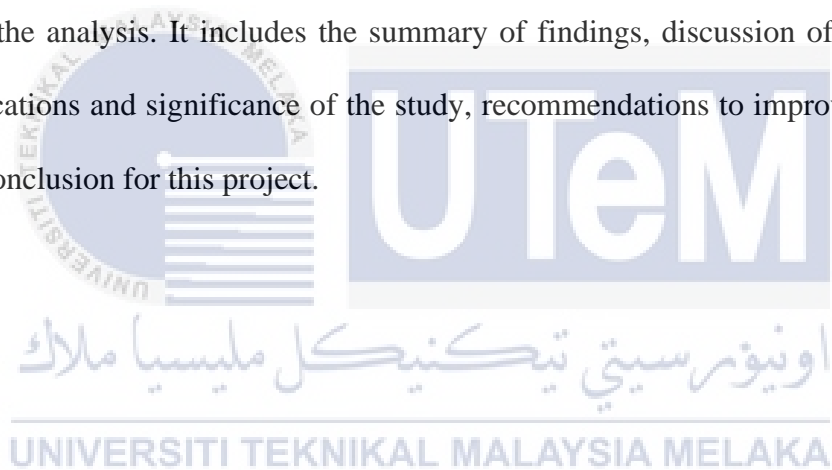
1.5 Thesis Outline

The first chapter, which is an introduction, sets the stage for a research paper or report and provides the reader with an overview of the study's objectives, scope, and problem statement. It serves as the first impression of the research and aims to capture the reader's attention while providing necessary background information.

The second chapter, which is background study provides the necessary context and foundation for understanding the research problem addressed in a report or research paper. It typically includes a comprehensive review of existing literature and relevant theories, providing a background understanding of the subject matter. The main purpose of this chapter is to establish the research's foundation and demonstrate the need for the current study. For methodology chapter, it describes the research approach, design, data collection methods, and evaluation methods employed in a study. It provides a detailed explanation of how the research was conducted, ensuring transparency, and allowing others to replicate or evaluate the study's validity.

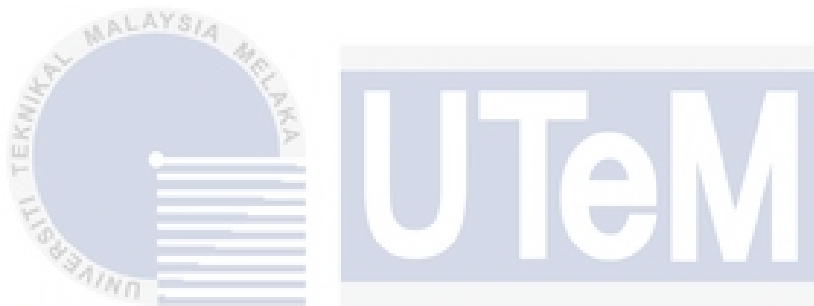
Next chapter, which is result and discussion presents the findings of a study and provides an in-depth analysis and interpretation of the results. This chapter aims to answer the research questions or test the hypotheses formulated in the earlier stages of the research. It consists of the I-V characteristic and response to the target gases of the gas sensor.

Finally, the conclusion and recommendation chapter are a vital section of any report or research paper as it summarizes the main findings and presents actionable recommendations future work based on the study's results. This chapter serves as a culmination of the research and offers a concise overview of the key insights derived from the analysis. It includes the summary of findings, discussion of key findings, implications and significance of the study, recommendations to improve this project and conclusion for this project.



CHAPTER 2

BACKGROUND STUDY



2.1 General Overview

The background study forms a critical component of research, providing an overview of existing knowledge and previous research conducted in the field. This section aims to establish the context, significance, and gaps in knowledge that the current research seeks to address. In previous research, a literature review from 11 journals by past researchers are being analyzed about the characteristics of Schottky junction gas sensor. It consists of the sensing material, deposition technique, electrode material, operating temperature, and target gases used in their research. The most material or criteria used by them is then being studied for a better understanding of why they are using such components in their research.

2.2 Previous Research on Schottky Junction Gas Sensor

Table 2.1 shows the characteristics of Schottky junction gas sensor by previous researchers. This table summarizes the key information about various sensing materials used for gas sensing applications, including the fabrication technique, electrode material, operating temperature, gases sensed, and the corresponding references for further details. According to previous research, Tin (IV) Oxide material are widely used as a sensing material for a gas sensor while gold, silver, and platinum are widely used as electrode material. For deposition technique, previous research heavily relied on hydrothermal, CVD, and thermal evaporation. The operating temperature for conducting the experiments was mostly room temperature. Nitrogen dioxide, carbon monoxide, and ammonia are widely used as the target gases based on previous researchers.

Table 2.1: Characteristics of Schottky junction gas sensor

| Sensing Material | Deposition Technique | Electrode material | Operating Temperature | Gas | Reference |
|--------------------------------|---------------------------|--------------------|-----------------------|--|-----------|
| Titanium dioxide/ Tin Oxide | Thermal evaporation | Gold | Room temperature | Nitrogen Dioxide | [1] |
| Tin Sulfide | Hydrothermal | Nickel | Room temperature | Ammonia | [2] |
| Graphene | Chemical vapor deposition | Titanium/ Gold | Room temperature | Nitrogen Dioxide, Ammonia, Carbon Monoxide | [3] |
| Tin Selenide | Hydrothermal | Gold | Room temperature | Ammonia | [4] |
| Gallium Nitride | Chemical vapor deposition | Platinum | 300 K | Hydrogen | [5] |
| Cadmium Sulfide | Thermal evaporation | Gold, silver | Room temperature | Carbon Monoxide, Nitrogen Dioxide | [6] |

| | | | | | |
|-----------------------------|-----------------------------------|----------|------------------|--|------|
| Tin (IV) Oxide | Thermal chemical vapor deposition | Gold | 200-300 °C | Acetone | [7] |
| Zinc Oxide/Titanium Carbide | Hydrothermal | Platinum | Room temperature | Nitrogen Dioxide | [8] |
| Indium (III) Oxide | Hydrolysis reaction | Silver | 120-240 °C | Formaldehyde (HCHO) | [9] |
| Tin (IV) Oxide | Hydrothermal | Silver | 180 °C | Ethanol | [10] |
| Tin dioxide | Screen printing | Platinum | 100-400 °C | Carbon Monoxide, Hydrocarbon, Nitrogen Oxide | [13] |

2.3 Schottky Junction

The Schottky barrier is the energy difference between the valence (or conduction) band edge of the semiconductor and the Fermi energy of the metal, while the band offset is the energy difference of valence (or conduction) bands of two materials that construct the interface [27]. Figure 2.1 shows the schematic diagram of Schottky barrier diode. Power diodes, also referred to as Schottky diodes, tend to be required to handle high voltages and/or currents with minimal power losses [29]. Specific requirements for recovery dynamics, breakdown voltage, forward-bias drop, reverse-bias current, and thermal impedance are also posed by the various application areas [29]. To maximize the benefits of the properties of the available materials and the new manufacturing technologies, device design is constantly changing [29].

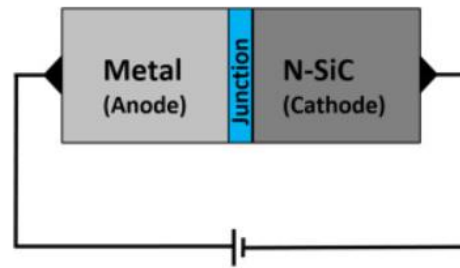


Figure 2.1: Schematic diagram of Schottky barrier diode [28]

2.3.1 Schottky Barrier Modulation

The carrier concentration and resistance of a composite material can be changed by applying a method called Schottky barrier modulation. This is done by changing the barrier height at the Schottky junction interface, which happens when a semiconductor and a metal come into contact under the right circumstances [31]. The oxygen molecules absorbed on the coated substrates can absorb free electrons from target materials and convert into oxygen anion O_2 when the gas sensor is exposed to air. This causes the composite's energy band to bend upward, the Schottky barrier to rise, and an electron depletion layer to form [32].

UNIVERSITI TEKNIKAL MALAYSIA MELAKA

2.4 Sensing Material for VOC Gases

Sensing materials for volatile organic compounds (VOCs) are essential for applications in healthcare, industry safety, and environmental monitoring. These materials are made to recognize and react to volatile organic compounds (VOCs), which can come from a variety of sources, including indoor pollutants, automobile emissions, and industrial processes. Gas sensors usually use particular materials that have intrinsic qualities that make it easier to detect volatile organic compounds

(VOCs) in a sensitive and selective manner. Because they enable the prompt and accurate detection of volatile organic compounds in a variety of settings, these sensing materials aid in the development of trustworthy and effective VOC gas sensors, promoting advancements in workplace safety, public health, and environmental protection. Effective VOC sensor creation requires careful consideration of material selection as well as sensor design and integration.

2.4.1 Tin (IV) Oxide (SnO_2)

Semiconductor composite materials, such as SnO_2 have been exploited as gas sensors for different gas due to their superior sensing performance [1]. SnO_2 is one of the most promising materials as a typical n-type semiconductor because of its high electron mobility and good stability [7]. The pristine SnO_2 sensor, however, typically has low selectivity and a high operating temperature [7]. Therefore, lowering the operating temperature of SnO_2 -based gas sensors and enhancing their sensing capabilities are crucial and difficult tasks [7]. Figure 2.2 shows the structure of pure SnO_2 .

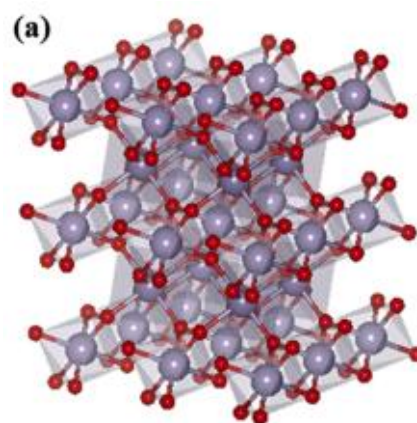


Figure 2.2: SnO_2 structure [14]

2.4.2 Graphene

Graphene, an atomically thin two-dimensional (2D) sheet of carbon atoms in a hexagonal lattice, has inspired a new era of research due to its exceptional properties such as extremely high mobility, very high thermal conductivity, surface sensitivity to various molecules, and so on [3]. However, due to its zero-band gap, graphene-based field effect transistors (FETs) have poor switching performance. Numerous studies have demonstrated that creating a heterojunction with graphene and another semiconductor can frequently solve this specific issue while also providing several additional advantages because the hetero interface has a non-negligible Schottky barrier [3]. Figure 2.3 shows the structure of pure graphene.

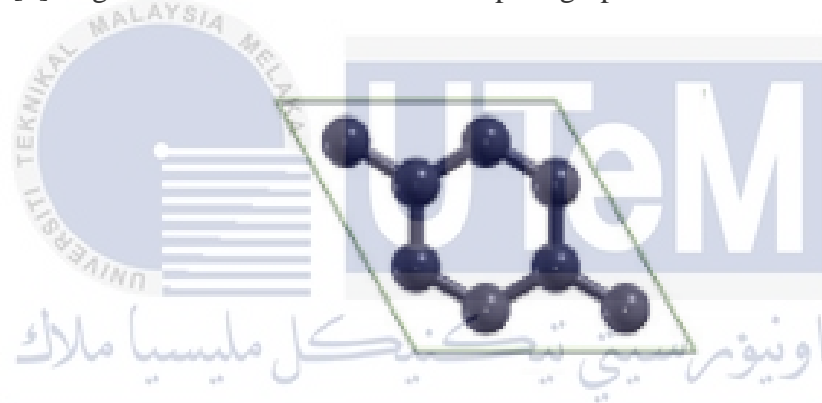


Figure 2.3: Graphene structure [15]

2.4.3 Titanium Dioxide (TiO₂)

TiO₂ (~3.2 eV) belongs to the wide-bandgap semiconductor, which has been studied as a promising gas sensing material owing to its excellent electron mobility and chemical stability [16]. The TiO₂ based gas sensors showed a good sensitivity to hydrogen, H₂ at 200 °C [16]. Titanium dioxide (TiO₂) is very promising due to its high specific surface, low cost, and robustness in chemical/corrosive atmosphere [17]. The challenge of insufficient sensing properties at room temperature still exists for TiO₂ based gas sensors [16]. The high working temperature, inadequate detection limit, and lengthy recovery time persist despite the numerous strengthened strategies that have

been suggested to improve sensitivity and selectivity [16]. Particularly, a high working temperature will cause grain size to increase and energy consumption to rise [16]. The fabrication of the sensors can be made easier as well as the stability of the sensing materials by reducing the working temperature [16]. Figure 2.4 shows the structure of TiO_2 .

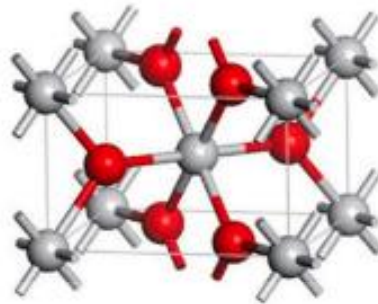


Figure 2.4: TiO_2 structure [18]

2.5 Deposition Technique for Gas Sensor

The processes used to coat or deposit thin films of sensing material onto substrates to form gas-sensitive layers are referred to as gas sensor deposition techniques. Because these layers interact with gases and produce a measurable response, they are essential for gas detection. Selectivity, sensitivity, and overall functionality are all impacted by this method. Researchers employ a range of techniques, each with unique benefits and drawbacks. The thin-film formation on substrates is influenced by the deposition technique selected, which in turn affects the sensor's capacity to identify and react to particular gases. It is essential to modify the fabrication process to fit the particular needs of the gas sensor application, taking into account elements like the desired sensing material properties, scalability, and substrate compatibility.

2.5.1 Chemical Vapor Deposition

Chemical vapor deposition is a term used to describe a method for depositing solid elements and compounds from gaseous molecular precursors [12]. Most of the elements in the periodic table can be deposited using a process called chemical vapor deposition, or CVD [12]. The temperature and cleanliness of the substrate are two of the critical aspects of the chemical vapor deposition (CVD) process [12]. Gas storage, flow, and recovery; byproduct scrubbers; reactor vessel composition and design are additional crucial elements [12]. This method of plating or coating requires clean, dry surfaces, which are essential for getting the best adhesion [12]. Using vapor degreasing or ultrasonic cleaning, residue from surfaces can be removed before they are ready for loading [12]. Any oxide coatings that may have developed on the surface are removed using reducing gases or mild acids while the material is being heated [12]. The reaction's critical substrate temperature must be stabilized throughout the process because it affects the outcome greatly [12]. If this doesn't happen, there's a chance that the film's structure, thickness, content, and properties will change [12].

Precursor quantity, temperature of the precursors and substrate, location of the precursors, separation between the precursors and substrate (especially when solid-state precursors are used), chamber pressure, flow rates, substrate and carrier gas types are the main growth parameters in a CVD system [19]. Figure 2.5 shows the operation of CVD technique.

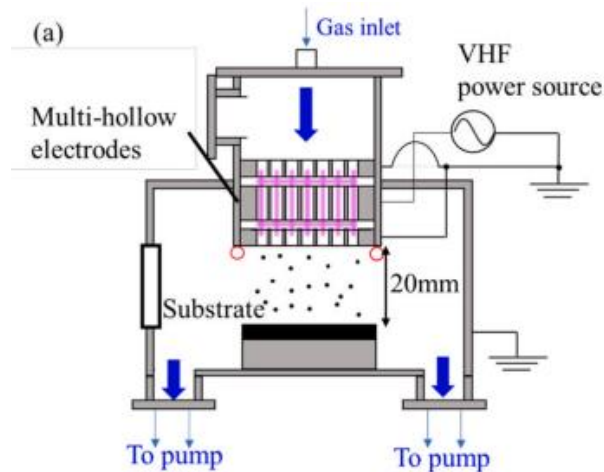


Figure 2.5: Chemical vapor deposition (CVD) technique [20]

2.5.2 Hydrothermal

One of the popular processes for creating nanomaterials is the hydrothermal process, which typically uses aqueous solutions as the reaction medium [21]. Water facilitates reactions that would otherwise be challenging under other conditions during hydrothermal processes [21]. In the liquid-phase hydrothermal (LPH) process, the reactants, additives, reagent ratios, temperature, and time are altered to produce the desired products [21]. However, consideration has been given to the environment outside the solution in the autoclave to prepare products with the precise structure and composition [21].

The vapor-phase hydrothermal (VPH) method was created because of the specimen's ability to react with gas molecules outside of the solution at high temperatures and pressures as shown in Figure 2.6 [21]. The hydrothermal method for depositing nanostructures is a desirable technique [22]. As a matter of fact, it offers many benefits, including ease of use, low cost, environmentally friendly conditions, and a wide range of flexibility to control the structure and morphology of the obtained nanostructures by altering the deposition conditions [22]. Aqueous solutions are

typically used for deposition [22]. As a result, the temperatures are lower than the water's boiling point [22].

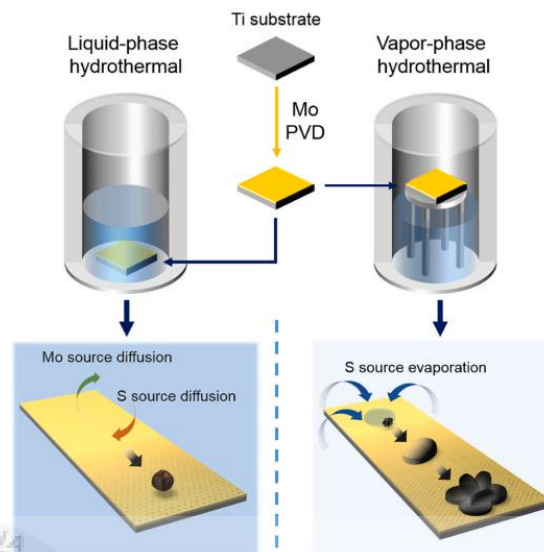


Figure 2.6: Hydrothermal technique [21]

2.5.3 Screen Printing

One of the most common printing techniques is screen printing, also known as serigraphy or silk-screen printing [23]. It has been regarded as the technique most frequently used for printing on fabric and paper [23]. Due to the pre-designed mesh patterns and the simple fabrication process, screen printing has been regarded as a highly competitive manufacturing technology for the scalable and quick fabrication of wearable microelectronics [25]. This method works by applying shear force through the mesh opening to deposit ink containing sensitive material on the substrate [25].

As a result, several factors, such as the preparation of the substrate, the choice of screen mesh, and the characteristic of the functional ink (such as rheology), affect the quality of screen-printed films [25]. Other factors can also be easily controlled during the printing process, except for ink rheology, which can be measured by measuring ink viscosity [25]. Therefore, like inkjet printing, careful thought should be given to

screen printing inks, which need to perform well and have the right rheology to accommodate a variety of application requirements [25].

The screen-printing technique can print various materials, such as carbon nanotubes and 2D materials, on a variety of substrates, such as textiles, paper, and glass, depending on the ink design and control of other parameters [25]. To create an imprint of a design through a stenciled mesh screen, the screen printer presses or pushes specialized ink onto a flat surface using a mesh screen, ink, and a squeegee [23]. For the fabrication of alternating or stacking microlayers, screen printing technology is very effective [24]. This technique is ideal for creating chemical sensors due to its exceptional qualities, which include low cost, simpler integration, versatility, portability, smaller sizes, and high electrical and thermal conductivity [23]. Figure 2.7 shows the screen-printing technique.

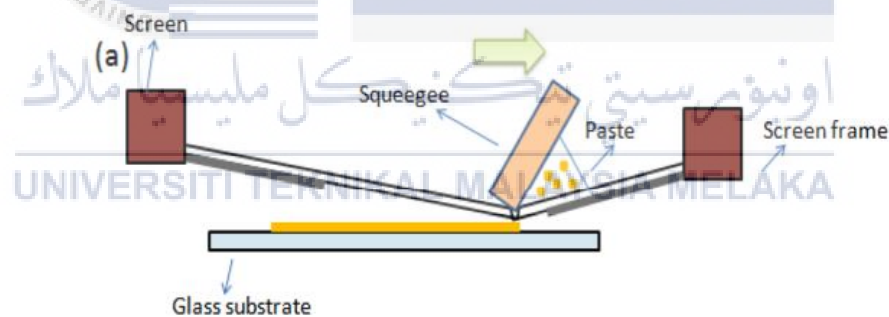


Figure 2.7: Screen printing technique [24]

2.6 Characteristics of Gas Sensor

Gas sensors are essential for identifying and tracking the presence of different gases in diverse settings, guaranteeing process efficiency and safety. The response of gas sensors, which gauges how well they react to the target gas, is one of their most

important features. While a fast response time is necessary for timely detection, a high response shows that a sensor can detect low concentrations. Sensitivity, or the sensor's capacity to recognize even minute variations in gas concentration, is another crucial factor. A sensor with high sensitivity can yield precise readings over a broad range of concentrations. Critical factors that affect how quickly a sensor responds to changes in gas levels and returns to its baseline state are response time and recovery time. For continuous monitoring, gas sensors should ideally have a short recovery time and a fast response time for real-time data.

2.6.1 Response

The response of a gas sensor is a critical factor in determining how well it detects particular gases. The gas sensing performance or response of the sensors was studied by measuring the current change in the presence and absence of the target gas. The response of the sensors on gas exposure is defined as [1]:

$$Response(s) = \left[\frac{I_{gas} - I_{air}}{I_{air}} \right] \times 100\%$$

I_{gas} is the current when the target gas is injected and I_{air} is the current when the target gas is replaced with dry air.

2.6.2 Sensitivity

The ability of gas sensors to identify low concentrations of a particular gas, or their reactivity to variations in gas levels, is referred to as sensitivity. It is a crucial feature that affects the sensor's dynamic range, measuring range, and detection threshold. Highly sensitive sensors are appropriate for applications where precision at low concentrations is crucial since they can identify even minute amounts of a target gas. To fully utilize gas sensors for accurate and dependable gas detection in a variety of

environments, however, high sensitivity and selectivity must be balanced with environmental influences, frequent calibration is necessary to preserve accuracy, and these factors must be taken into account.

2.6.3 Response Time and Recovery Time

The amount of time it takes a gas sensor to notice and react to changes in gas concentration is known as response time. For real-time monitoring applications where prompt detection of gas leaks or environmental changes is necessary, quick response time is essential. For recovery time, a crucial property of gas sensors gauges how long it takes a sensor to return to its initial state following exposure to a target gas. It is particularly important in applications that call for ongoing monitoring or repeated measurements. A gas sensor's recovery time is the amount of time it takes for it to reach its baseline reading after being exposed to a target gas. It reveals how quickly the sensor regains its sensitivity and stabilizes.

The proposed bias scheme for the PBR is shown in Figure 2.8, where $|VPBR|$ is the pulse amplitude [26]. Gas molecules adsorbed in the sensing material channel receive a strong electric field in the opposite direction of the bottom-gate when a strong negative voltage pulse is applied to the gate [26]. The sensor can then be quickly recovered after the electric field has desorbed the gas molecules [26]. By applying pulsed biases with a 10 ms width, the sensor is fully recovered using this pulse bias scheme [26].

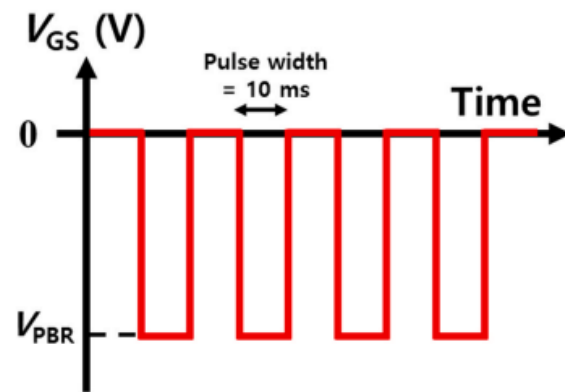


Figure 2.8: Response and recovery time using pulsed bias recovery (PBR) [26]

CHAPTER 3

METHODOLOGY



3.1 General Overview

This chapter contains the methodology for the investigation of TiO₂/Graphene Schottky junction for VOC gases. Each process will be explained as shown in this chapter. This includes the design structure of the gas sensor, preparation of the binder and paste, fabrication of the gas sensor, and the experimental setup to obtain the I-V characteristics and experimental setup when exposing to target gases such as acetone and ethanol for collecting data response of the TiO₂/graphene gas sensor. The detail of the setup will be reviewed at the end of this chapter.

3.2 Methodology Flowchart

The methodological approach to investigate the titanium dioxide/graphene Schottky junction for volatile organic compound gases is by researching about the Schottky characteristic. The structure is drawn by using the structure of Schottky junction gas sensor proposed by past researchers. Then the binder will be prepared to bind the titanium dioxide/graphene onto Kapton film. Next is the preparation of the titanium dioxide/graphene paste using 3 different ratios to get the suitable paste that can response to the ethanol and acetone vapor. This Schottky junction structure consists of two layers which are sensing material and electrode that will be deposited using screen printing technique. Then the Schottky junction design will be tested with I-V characteristic for its responsiveness to ethanol and acetone gases. Figure 3.1 shows the flowchart of this project.



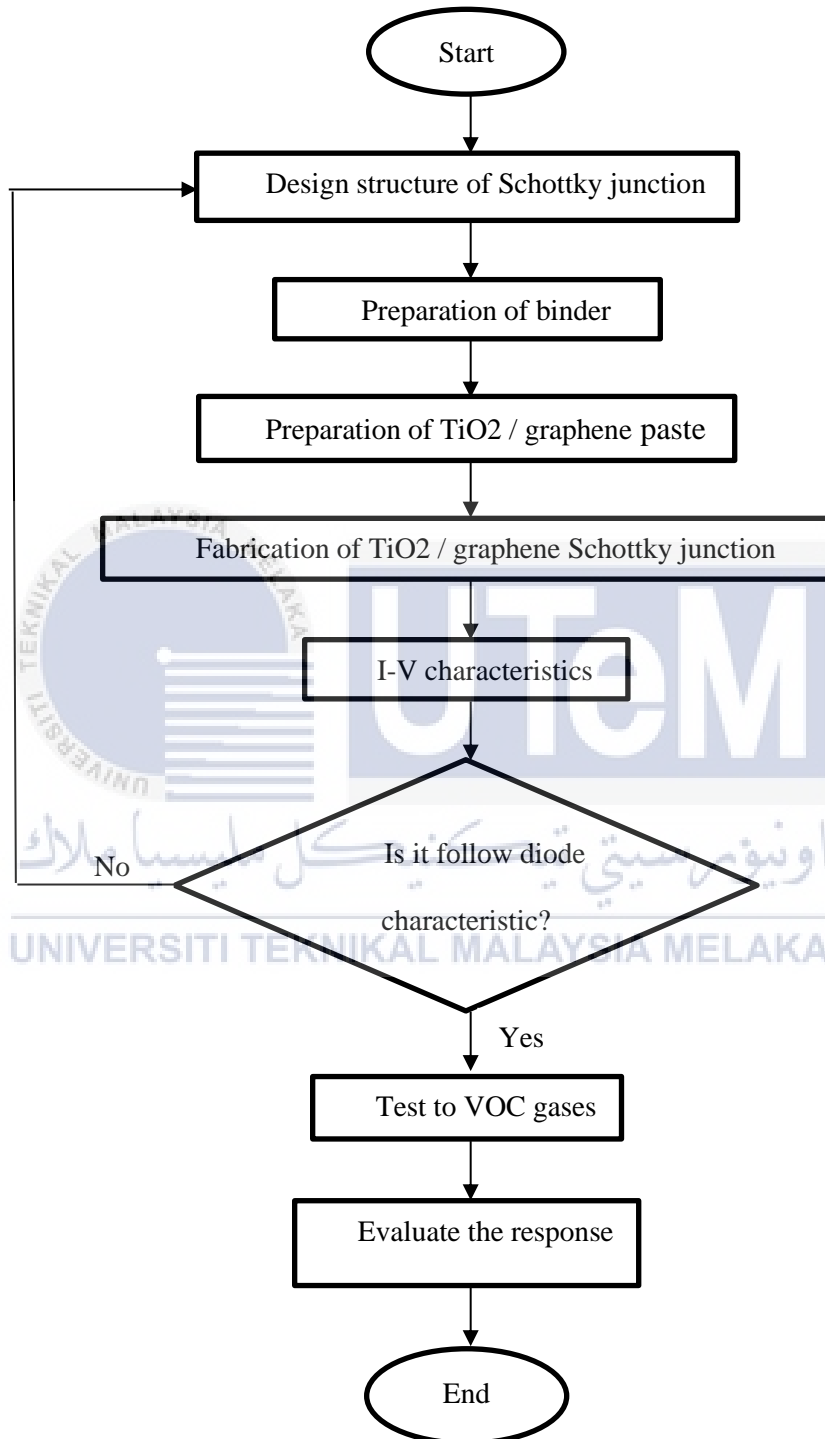


Figure 3.1: Research methodology flowchart

3.3 Design Structure of Schottky Junction

The structure is drawn by using the structure of Schottky junction gas sensor proposed by past researchers using AutoCAD software. There are three designs that are drawn as shown in Figure 3.2. To achieve Schottky diode characteristic, this design is created to ensure which can meet the criteria of a Schottky diode. Figure 3.2 (a) is the structure design that has been used by past researcher [6] and Figure 3.2 (c) is the structure design by another researcher [3]. The annotation in Figure 3.2, 3.3, and 3.4 is in millimeters. After that, the structure will be separated according to the type for sensing material and electrode. The design of the structure will be printed on two stencils for screen printing deposition purposes. Figures 3.3 and 3.4 show the layout of the sensing material and electrode dimensions on the stencils for each design respectively. Table 3.1 shows the area of electrode and sensing material for design 1, design 2, and design 3. Each design has different size of sensing material and electrode. Design 3 has bigger area in terms of electrode which is 2.4 cm^2 compared to the others while design 1 has the biggest area in terms of sensing material which is 2.56 cm^2 . Overall, design 1 has 3.14 cm^2 , design 2 has 3 cm^2 while design 3 has 4 cm^2 in term of the size of $\text{TiO}_2/\text{graphene}$ the gas sensor.

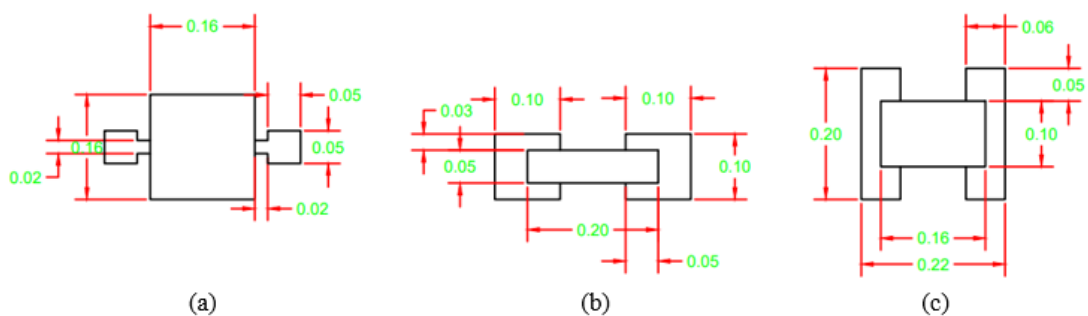


Figure 3.2: 2D structure design of Schottky Junction in top view (a) Design 1, (b) Design 2, and (c) Design 3

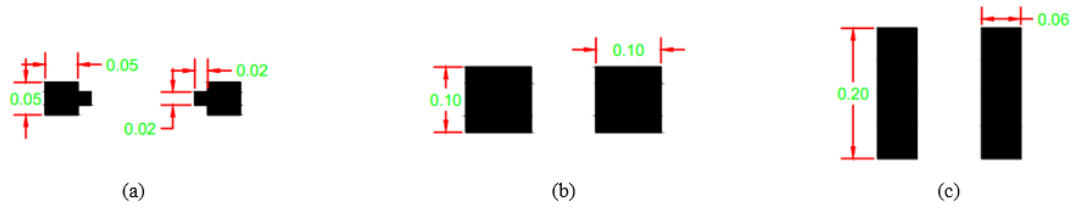


Figure 3.3: Layout of Sensing Material (a) Design 1, (b) Design 2, and (c) Design 3

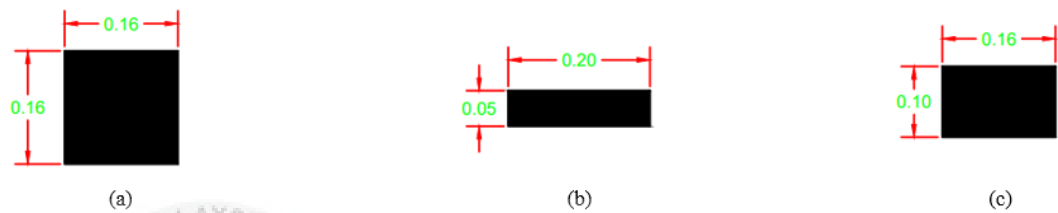


Figure 3.4: Layout of Electrode (a) Design 1, (b) Design 2, and (c) Design 3

Table 3.1: Area (cm²) of design

| Design | Area (cm ²) | |
|--------|-------------------------|------------------|
| | Electrode | Sensing Material |
| 1 | 0.58 | 2.56 |
| 2 | 2.00 | 1.00 |
| 3 | 2.40 | 1.60 |

3.4 Preparation of Binder

There are three materials that are used to make a binder as shown in Figure 3.5 (a). The materials are 2 wt% ethyl cellulose, 5 wt% linseed oil, and 93 wt% terpineol for the ratio of each material. These materials will be mixed in a vial according to their ratio and a magnetic bar will be inserted as shown in Figure 3.5 (b). The vial will then

be placed on a magnetic stirrer with settings of 40°C and 200 rpm for at least 24 hours to get a proper binder as shown in figure 3.5 (c). The binder cannot be used after six months. Therefore, a new binder will be prepared if there is a need to use more binder. Figure 3.5 (d) shows the final product of the binder after it's been stirred for more than 12 hours.

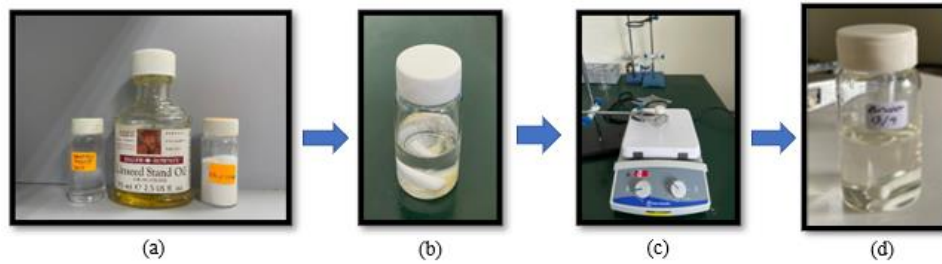


Figure 3.5: Process of making binder (a) Ethyl cellulose, Linseed oil, Terpeneol, (b) Before stir, (c) Stirring process, and (d) Binder

3.5 Preparation of TiO₂/Graphene Paste

TiO₂/graphene paste is prepared using three different ratios. To prepare the first paste, TiO₂ and graphene are added with a ratio of 99 wt% and 1 wt% respectively. For the second paste, TiO₂ and graphene are added with a ratio of 98 wt% and 2 wt% respectively. For the third paste, TiO₂ and graphene are added with a ratio of 95 wt% and 5 wt% respectively. Table 3.2 shows the ratio of each paste.

Table 3.2: Ratio for TiO₂/graphene paste

| Paste | TiO ₂ (wt%) | Graphene (wt%) |
|-------|------------------------|----------------|
| 1 | 99 | 1 |
| 2 | 98 | 2 |
| 3 | 95 | 5 |

Figure 3.6 shows the process for making TiO₂/graphene paste. TiO₂ and graphene have been used to prepare the paste. By using analytical balance, the weight of each material will be measured as shown in Figure 3.6 (a). After that, 25 ml of acetone will be added into the beaker containing the TiO₂ and graphene as shown in Figure 3.6 (b). Then the solution will be placed into an ultrasonic cleanser for 10 minutes with the temperature of 40°C for sonication process as shown in Figure 3.6 (c). Then the solution will be placed inside an oven at a temperature of 100°C until it becomes powder. Figure 3.6 (d) shows the picture of the oven that is been used. Figure 3.6 (e) shows the solution of paste that has become powder. Then the powder will be grinded gently in a mortar using pestle until they are even as shown in Figure 3.6 (f). Figure 3.6 (g) shows the paste powder that has been grinded using the pestle. Next, the weight of the powder will be measured using analytical balance because the ratio for TiO₂/graphene powder is 55 wt% while binder is 45 wt%. The weight of binder needs to be calculated beforehand based on the weight of TiO₂/graphene powder. Then the powder will be added into the binder little by little to get a smooth mixture while stirring it on the magnetic stirrer. The magnetic stirrer is set for 40°C and 80 rpm and will run for at least 24 hours. Figure 3.6 (h) shows the stirring process of the paste. Finally, the final product of TiO₂/graphene paste is shown in Figure 3.6 (i). Figure 3.7 show each ratio of paste after grinding process while Figure 3.8 shows the TiO₂/graphene paste for each ratio.

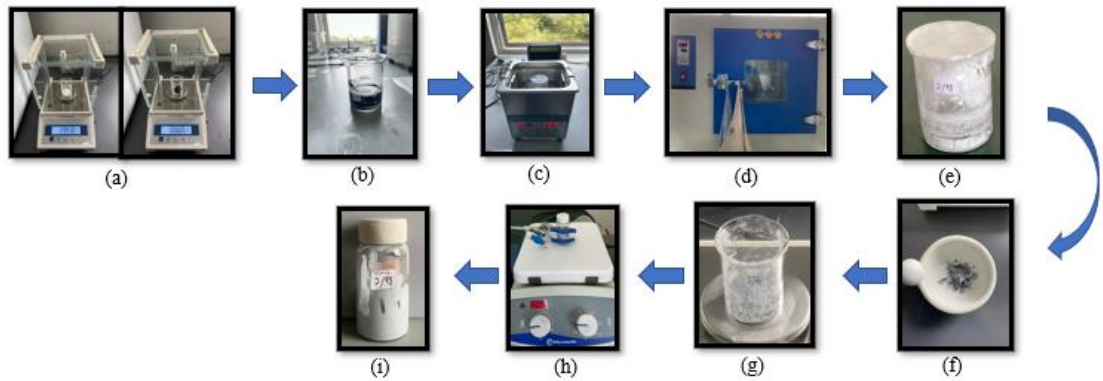


Figure 3.6: Preparation of TiO_2 /graphene paste (a) TiO_2 and graphene, (b) Adding 25 ml acetone, (c) Sonication process, (d) Heating process, (e) After heating process, (f) Grinding process, (g) TiO_2 /graphene powder, (h) Stirring process, and (i) TiO_2 /graphene paste

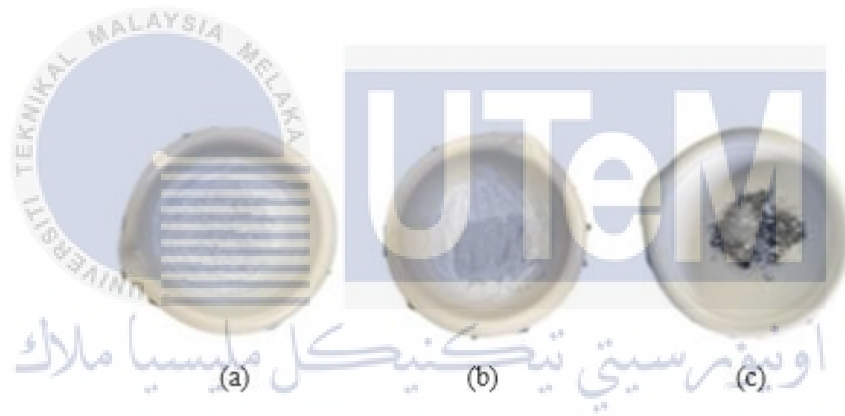


Figure 3.7: Powder of each paste before adding binder (a) T99_G1, (b) T98_G2, and (c) T95_G5



Figure 3.8: TiO_2 /graphene paste

3.6 Fabrication of TiO₂/Graphene Schottky Junction

The substrate for the gas sensor was made of Kapton film. This substrate was cut into the size of 4.0 cm x 4.0 cm in many pieces. These substrates will then be used for the deposition process.

3.6.1 Electrode Deposition

Figure 3.9 shows the flow process of depositing electrode onto substrate. The deposition technique used in this project is screen-printing technique. Silver, an electrode was deposited onto the substrate using screen-printing techniques. Electrode is placed on the stencil and squeegee were used to print the silver onto the substrate as shown in Figure 3.9 (a). Figure 3.9 (b) shows an example of a substrate that has undergone deposition process before heating process in Figure 3.9 (c) while Figure 3.9 (d) shows the substrate after heating process. The electrode must be heated in an oven with temperature of 150°C for 15 minutes.

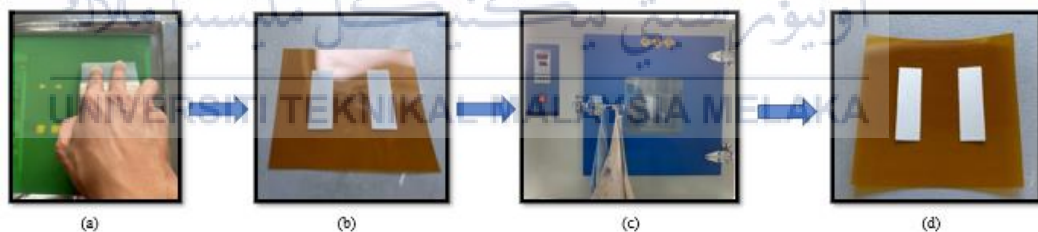


Figure 3.9: Electrode deposition (a) Printing process, (b) Before heating, (c) Heating process, and (d) After heating

3.6.2 Sensing Material Deposition

For the sensing material which is TiO₂/graphene paste, it was deposited onto the substrate using screen-printing techniques as shown in Figure 3.10 (a). The TiO₂/graphene paste is placed on the sensing material stencil and squeegee were used to deposit the sensing material onto the substrate with an electrode. Figure 3.10 (b) shows the sensing material deposited onto the substrate before the heating process as

shown in Figure 3.10 (c) while Figure 3.10 (d) shows the sensing material after heating process. The sensing material must be heated in an oven with temperature of 200°C for 1 hour.

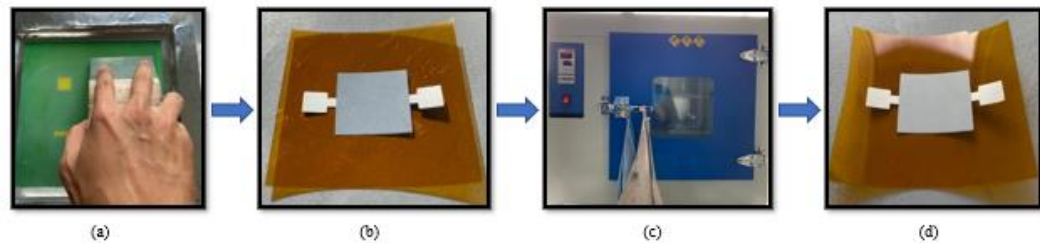


Figure 3.10: Sensing material deposition (a) Printing process, (b) Before heating, (c) Heating process, and (d) After heating

Finally, copper wire with length of 3 cm as shown in figure 3.14 were added onto the substrate. Before that, the copper wire is rubbed using sandpaper to remove the impurities of the wire. Then, the copper wire is stuck onto the electrode using silver paste and heated at 150°C for 15 minutes.

اونيورسيتي تيكنيكل مليسيا ملاك

UNIVERSITI TEKNIKAL MALAYSIA MELAKA

3.7 I-V Characteristics

Figure 3.11 shows the setup of current-voltage (I-V) measurement. It consists of the gas chamber, picoammeter, and computer. The source meter (Keithley 6487) was used to supply voltage to the gas sensor, which was housed in a gas chamber. Before the gas sensor is exposed to the target gases, I-V measurement is needed to check the conductivity of the fabricated gas sensor. The output current of the gas sensor is then recorded using LabVIEW 2010 software on the computer. The I-V measurement is recorded from 1V until 11V which is the breakdown voltage of the gas sensor [34].

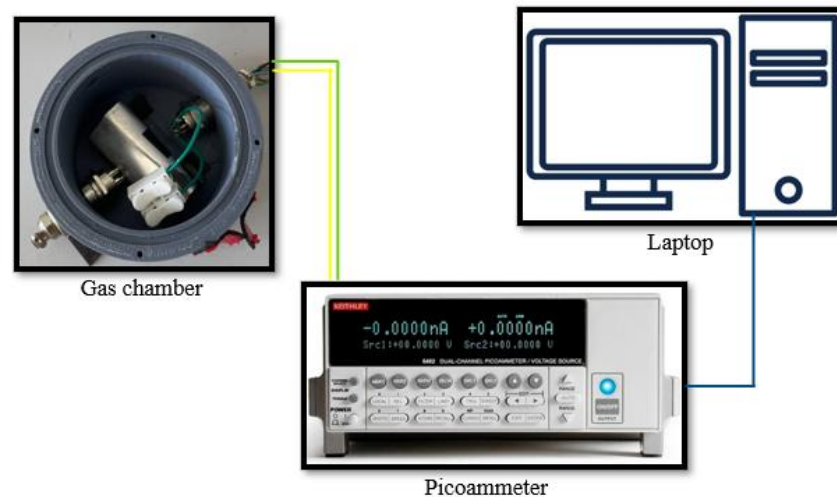


Figure 3.11: I-V measurement of the gas sensor

3.8 Experimental Setup of Gas Sensor to Ethanol and Acetone

Figure 3.12 shows the experimental setup of gas sensor measurement to target gases. The chamber is used to house the gas sensor. Acetone and ethanol are evaporated in glassware, and a silicone hose is used to pump the vapor into the gas chamber. With a magnetic stirrer set to 100 rpm, 25 ml of each solution was combined with 25 ml of distilled water to create the two solutions. The solution is then heated to a temperature of 120°C for 30 minutes to produce acetone and ethanol vapor. At first, it took 10 minutes for the gas sensor's current to stabilize at standard atmospheric pressure. The response value was then monitored within 30 minutes of acetone and ethanol vapor being connected to the gas chamber's inlet. The glassware's connection to the gas chamber was severed after 30 minutes, leaving another 10 minutes for the $\text{TiO}_2/\text{graphene}$ gas sensor to stabilize. Using Origin 2022 software, all the data obtained from LabVIEW 2010 were plotted [35].

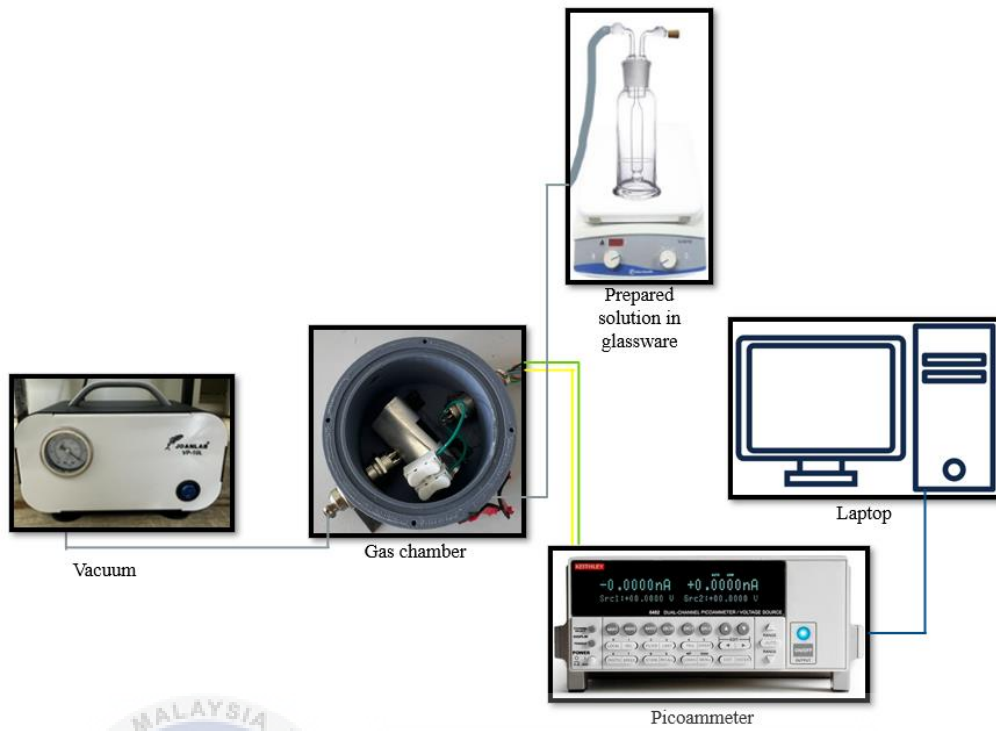


Figure 3.12: Experimental setup of gas sensor measurement

CHAPTER 4

RESULTS AND DISCUSSION

4.1 General Overview

This chapter offers a thorough examination of a manufactured gas sensor, highlighting its overall performance and I-V characteristics. After providing an overview of the basic concepts of gas sensing, the chapter concentrates on explaining the behavior of the sensor by analyzing its current-voltage. In order to assess the dependability of the sensor, performance evaluation criteria such as response are covered. Experimental results are used to illustrate practical application, with a focus on the sensor's reaction to acetone and ethanol concentrations of 25 ml. This thorough summary opens the door for improvements in sensor design and optimization by fostering a broader awareness of gas sensing technologies and their possible uses.

4.2 Fabrication of Gas Sensor

There are three designs of the gas sensor. Each design will be printed on a Kapton film using TiO_2 /graphene paste. T99_G1 paste contain 99 wt% TiO_2 and 1 wt% graphene, T98_G2 contain 98 wt% TiO_2 and 2 wt% graphene and T95_G5 contain 95 wt% TiO_2 and 5 wt% graphene. Figure 4.1 shows the sample of 4 cm x 4 cm gas sensor with different type of paste and design. If the amount of graphene increase, the colour of the paste will become darker. The difference in colour of the sensing material paste can be seen in Figure 4.1. Figure 4.1 (c), (d), and (i) is darker because there is 5 wt% graphene compared to the others. This is because graphene powder used is in black colour while TiO_2 powder has white colour.

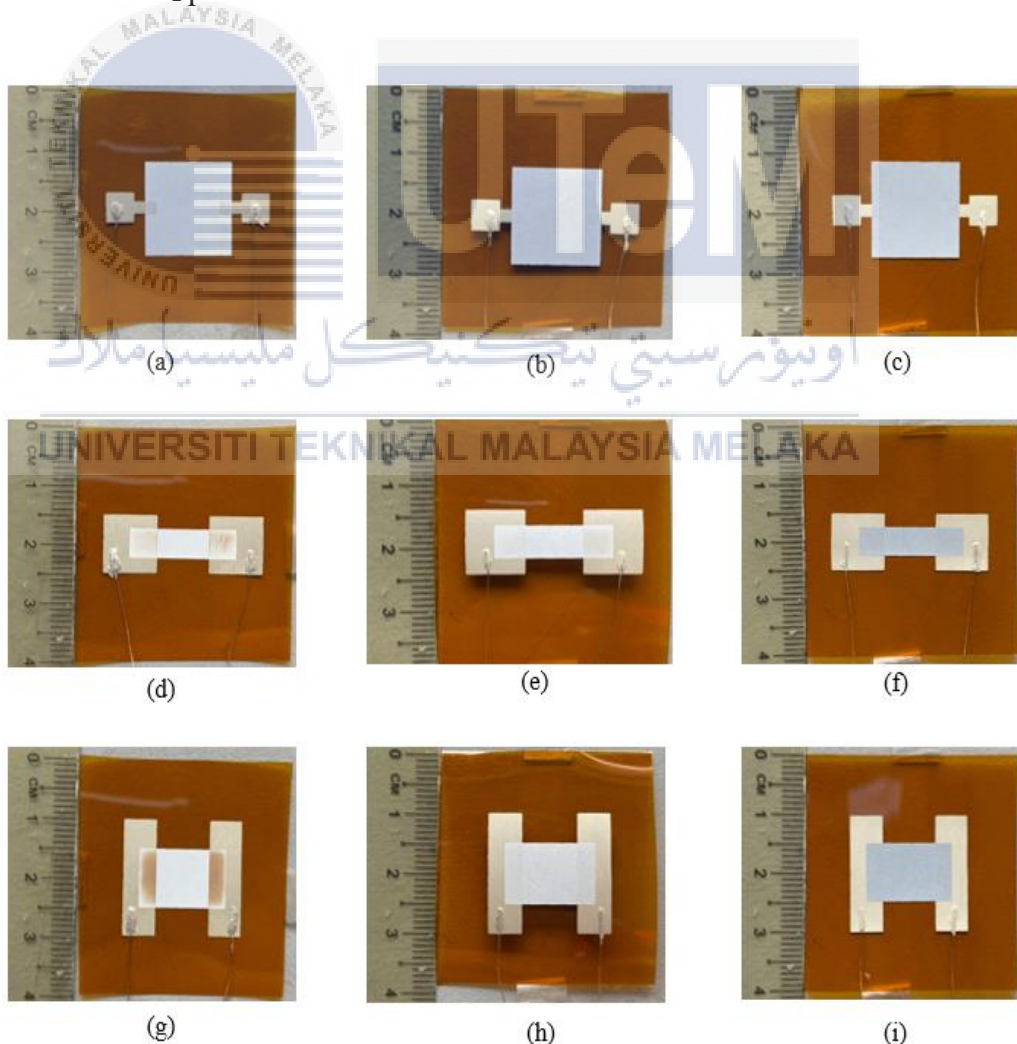


Figure 4.1: Fabricated TiO_2 /graphene (a) T99_G1_1, (b) T98_G2_1, (c) T95_G5_1, (d) T99_G1_2, (e) T98_G2_2, (f) T95_G5_2, (g) T99_G1_3, (h) T98_G2_3, and (i) T95_G5_3

4.3 I-V Characteristics

An essential metric for determining how a gas sensor will react to variations in gas concentration is its current-voltage (I-V) characteristic, which shows the relationship between the applied voltage and the generated current. It displays how the electrical behavior changes with different amounts of gas. The sensor displays a baseline current and voltage, which represents its typical state, when the target gas is not present. The I-V characteristic shows changes in the electrical characteristics of the sensor upon exposure to the target gas, suggesting an increase or reduction in current depending on the sensing method.

Based on the result of past researcher, for Schottky diode current-voltage measurements, the capacitance at forward bias should remained constant over the whole voltage range. Since a totally depleted layer can be used to explain this, it is plausible to infer that the depletion width is comparable to the thickness of the organic layer. Thus, for a minimal value of the depletion width, an upper limit can be calculated for the p-type doping in the organic layer. Upper limit values should be found for the mobility of the charge carriers in the organic layer and the concentration of p-type doping [30].

The Schottky junction structures were intentionally designed with the unexpected outcome of deviating from the typical diode I-V characteristic, showcasing a distinctive linear I-V profile reminiscent of resistors. However, all of the design produces linear graph for the current-voltage measurement. This is because the biasing conditions does not fulfilled. The correct biasing conditions must be applied to observe the Schottky behavior. The Schottky diode typically shows rectifying behavior under forward bias and higher resistance under reverse bias. Figure 4.2 shows the I-V

characteristics at 1V for each sample design using three different pastes fabricated gas sensor on Kapton film. Based on Figure 4.2, (a) and (c) produce more linearity compared to (b).

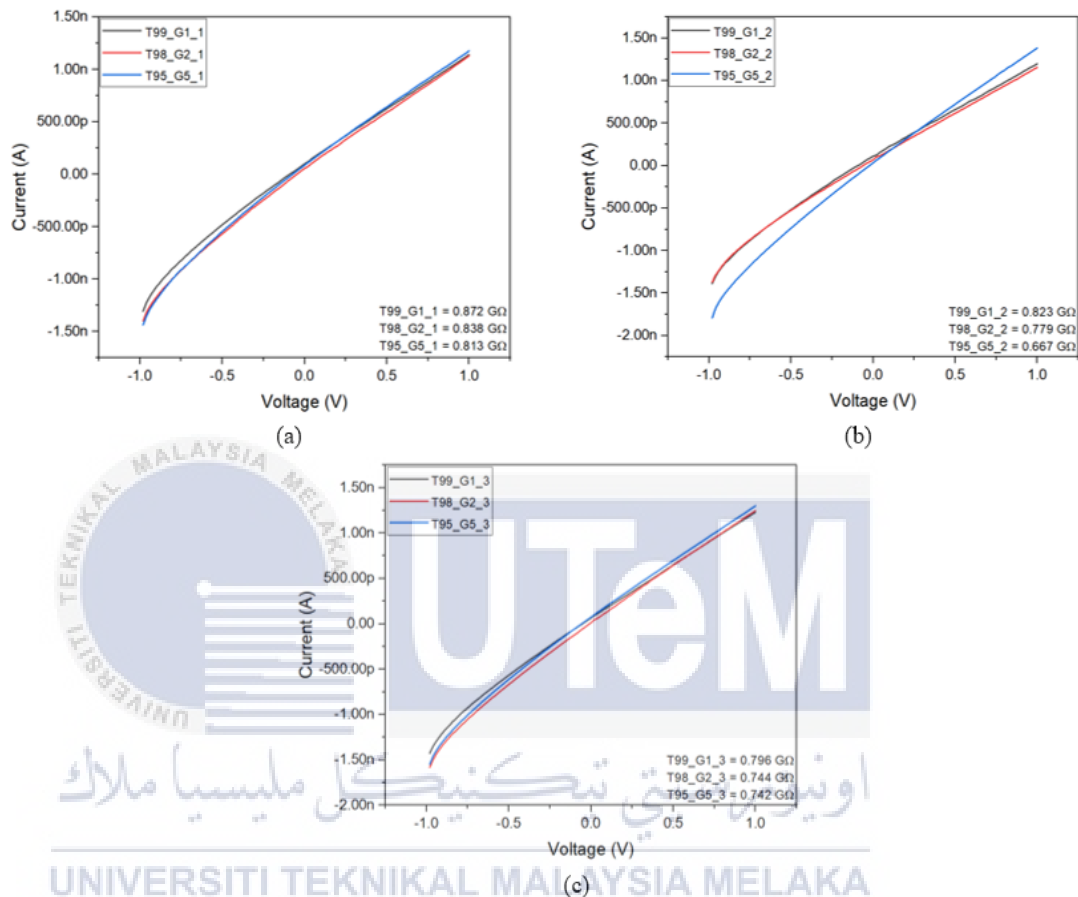


Figure 4.2: I-V characteristic (a) Design 1 (b) Design 2 (c) Design 3

The resistance value is shown in Table 4.1. The value of resistance is decreasing with each paste. This is due to the amount of graphene in the sensing material. Because of graphene's exceptional electrical conductivity, variations in its concentration can affect the resistance of the sensor. Aside from that, the quantity of silver paste utilized to adhere the copper wire to the electrode leg can affect the gas sensor's resistance. This means that the lower the amount of graphene in a paste, the higher the resistance value of the gas sensor will become. Because of two different parameters which is the

size of electrode and sensing material, it is hard to differentiate the cause of resistance value that varied between each design. The area of each design is varied. Design 1 has 3.14 cm^2 , design 2 has 3 cm^2 while design 3 has 4 cm^2 . Design 1 has 0.841 Gohm average value resistance while design 2 and 3 has 0.756 and 0.761 Gohm respectively. The result revealed that the area of sensing material can influence the value of resistance in a gas sensor. Because of design 1 bigger area in term of sensing material, the value of resistance is higher compared to design 2 and 3. More places for gas molecules to interact with the sensing material can be created by increasing its surface area. When exposed to the target gas, this may cause a more noticeable alteration in the material's electrical characteristics. The sensitivity of the sensor also may be improved by a greater surface, enabling it to detect gas concentrations that are lower.

The size of electrode can also affect the value of resistance because design 1 has the smallest area while design 3 is the biggest. More contact points with the sensing material can be made possible by a larger electrode area, which will improve the electrical connection overall. By doing this, resistive losses may be decreased and resistance changes may be measured with greater accuracy and dependability. Reducing resistive losses also is essential for precise and trustworthy measurements, particularly when identifying minute variations in resistance brought on by changes in gas concentration. A material's resistance and conductivity are inversely correlated. Greater conductivity is indicated by lower resistance. Changes in gas concentration cause changes in the sensing material's conductivity or resistance in the context of gas sensors. Greater electrical contact between the electrodes and the sensing material may result in lower resistive losses with larger electrodes. As shown in Table 3.1, the area size of electrode for design 1 is smaller compared to others which is 0.58 cm^2 and

Table 4.1 shows the result of the resistance value. T99_G1_1 has the highest resistance which is 0.872 Gohm.

Table 4.1: Resistance value for each design of sample and paste

| Design | Sample name | Resistance (Gohm) |
|--------|-------------|-------------------|
| 1 | T99_G1_1 | 0.872 |
| | T98_G2_1 | 0.838 |
| | T95_G5_1 | 0.813 |
| 2 | T99_G1_2 | 0.823 |
| | T98_G2_2 | 0.779 |
| | T95_G5_2 | 0.667 |
| 3 | T99_G1_3 | 0.796 |
| | T98_G2_3 | 0.744 |
| | T95_G5_3 | 0.742 |

4.4 Performance of Gas Sensor

The response characteristics of a gas sensor are one of the most important factors taken into consideration when evaluating its performance. A gas sensor's response is defined as its capacity to identify and react to the presence of a particular gas or gases. To get the response for each fabricated TiO₂/graphene gas sensor, it will be exposed to the target gases such as acetone and ethanol. By using the experimental setup as shown in chapter 3, the response value for each sample of gas sensor is recorded. This process took 50 minutes in total to complete one sample. It is divided into three part which is exposed to air for 10 minutes, target gases for 30 minutes, and another 10

minutes after removing the target gases. The experiment is carefully done to reduce the undesired changes or oscillations in the sensor's output signal that are not indicative of the real gas concentration being measured referred as signal noise.

4.4.1 Response to 25ml Acetone

Figure 4.3 shows the graph response for design 1, 2 and 3 to acetone gas for each paste which is T99_G1, T98_G2, and T95_G5 respectively. The first 10 minutes is exposing TiO₂/graphene gas sensor at atmospheric pressure without the presence of acetone gas to achieve stability. After it has been stable, the acetone gas will be connected to the inlet of the gas chamber that contain fabricated TiO₂/graphene gas sensor for 30 minutes and vacuum will be turned on. After that, the acetone gas hose is removed from the gas chamber to make the gas sensor stable again.

Based on Figure 4.3, when the gas sensor detects the presence of acetone gas, the current will increase and resistance will decrease. This indicate that the fabricated TiO₂/graphene gas sensor has response toward acetone gas. All sample exposed to the acetone gas has the same graph trend with past researcher which are using TiO₂ as sensing material to detect acetone gas [33]. Current is increasing when the gas sensor exposed to acetone gas. Acetone molecules adsorb and desorb from the surface of TiO₂ during the interaction between the two substances. The conductivity and other properties of the TiO₂ material may be impacted by this process.

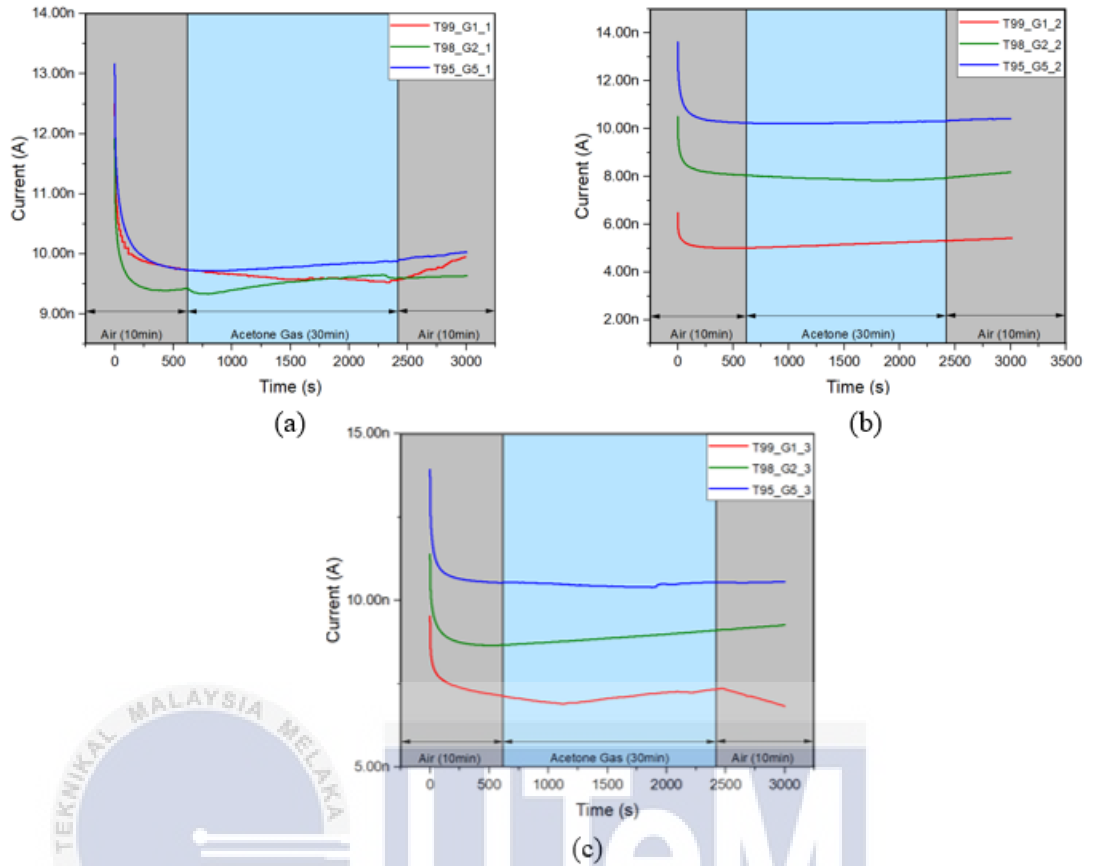


Figure 4.3: Response of TiO₂/graphene gas sensor to acetone vapor (a) Design 1 (b) Design 2 (c) Design 3

Table 4.2 shows the response value for each sample that has been exposed to acetone gas. All of the samples have a response toward acetone gas. For design 1, T98_G2_1 has higher response which is 1.0182 followed by T95_G5_1 and T99_G1_1 which has 1.0147 and 1.0021 respectively. This resulting in 2 wt% graphene has higher response to acetone gas.

For design 2, T99_G1_2 has higher response to acetone gas which is 1.0605 compared to paste 2 and 3 which has the response value of 1.0001 and 1.0059 respectively. For this design, using 1 wt% graphene is more compatible in detecting acetone gas.

For design 3, T98_G2_3 has higher response to acetone gas with the value of 1.0509 compared to paste 1 and 3 which has 1.0255 and 1.0001 respectively. Overall, design 2 using TiO₂ 99 wt% and 1 wt% graphene has the best response toward acetone gas but design 3 has the highest average response value which is 1.0255 compared to design 1 and 2 which has 1.0117 and 1.0222 respectively. This is due to larger electrodes and sensing material give gas molecules more surface area to interact with. More gas molecules can be adsorbed onto this larger surface area, which can increase the sensor's sensitivity by causing a more noticeable change in its electrical characteristics.

Table 4.2: Response value to acetone gas

| Design | Sample name | Response |
|--------|-------------|----------|
| 1 | T99_G1_1 | 1.0021 |
| | T98_G2_1 | 1.0182 |
| | T95_G5_1 | 1.0147 |
| 2 | T99_G1_2 | 1.0605 |
| | T98_G2_2 | 1.0001 |
| | T95_G5_2 | 1.0059 |
| 3 | T99_G1_3 | 1.0255 |
| | T98_G2_3 | 1.0509 |
| | T95_G5_3 | 1.0001 |

4.4.2 Response to 25ml Ethanol

The graph response for designs 1, 2, and 3 to ethanol gas for each paste T99_G1, T98_G2, and T95_G5 is displayed in Figure 4.4. In order to achieve stability, the

TiO₂/graphene gas sensor is exposed for the first ten minutes at atmospheric pressure without the presence of ethanol gas. Once it is stable, the ethanol gas will be connected for 30 minutes to the gas chamber's inlet, which houses the manufactured TiO₂/graphene gas sensor, and the vacuum will be activated. To restore the gas sensor's stability, the ethanol gas hose is then taken out of the gas chamber.

Based on Figure 4.4, when the gas sensor detects the presence of ethanol gas, the current will increase and resistance will decrease. This indicate that the fabricated TiO₂/graphene gas sensor has response toward ethanol gas. All sample exposed to the acetone gas has the same graph trend with past researcher which are using TiO₂ as sensing material to detect ethanol gas [33]. Current is increasing when the gas sensor exposed to acetone gas. Acetone molecules adsorb and desorb from the surface of TiO₂ during the interaction between the two substances. The conductivity and other properties of the TiO₂ material may be impacted by this process.

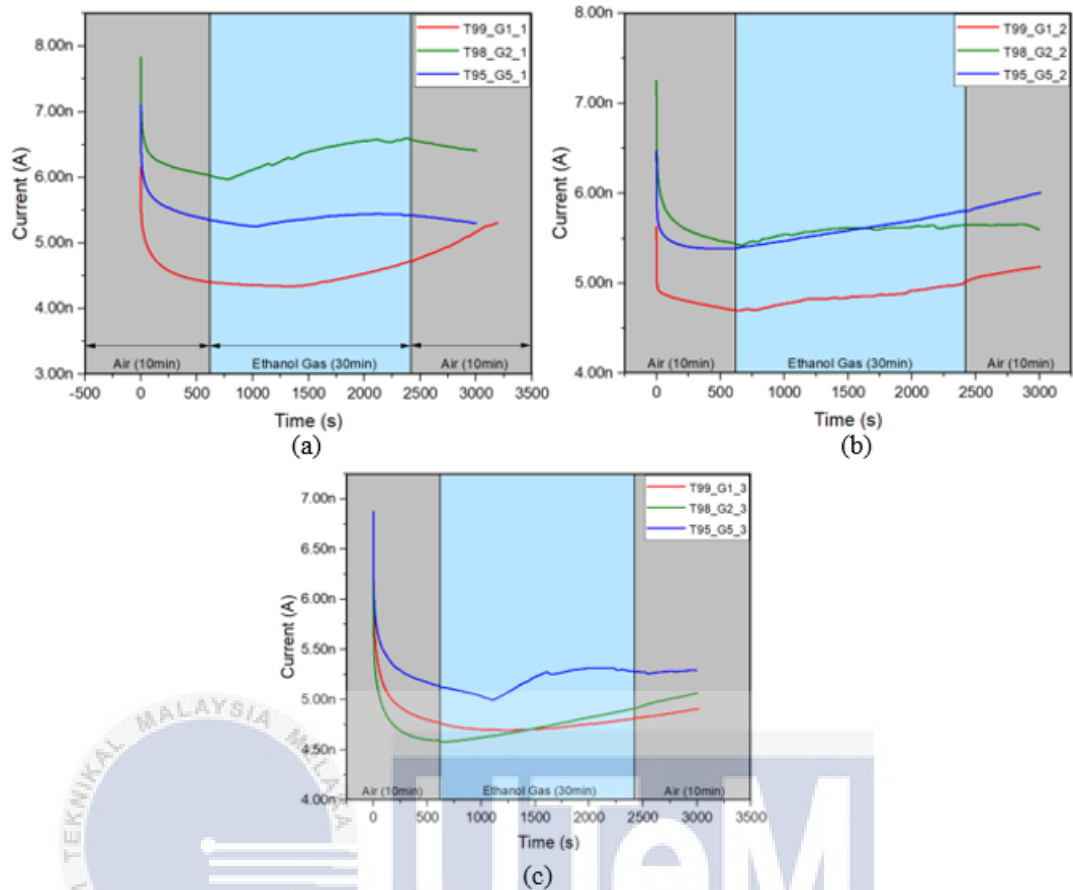


Figure 4.4: Response of TiO₂/graphene gas sensor to ethanol vapor (a) Design 1 (b) Design 2 (c) Design 3

The response value for each sample exposed to ethanol gas is displayed in Table 4.3. Every sample reacts differently to ethanol gas. With a higher response of 1.0906 for design 1, T98_G2_1 is in front of T99_G1_1 and T95_G5_1, with 1.0698 and 1.0126, respectively. As a result, the response of 2 wt% graphene to ethanol gas is higher.

When it comes to design 2, T95_G5_2 responds to ethanol gas more strongly (1.0777) than pastes 2 and 3, which have response values of 1.0616 and 1.0366, respectively. Detecting ethanol gas is more compatible with this design when 5 wt% graphene is used.

With a value of 1.0669, T98_G2_3 for design 3 responds to ethanol gas more strongly than pastes 3 and 1, which have values of 1.0276 and 1.0073, respectively. In general, design 1 exhibits the best response to ethanol gas using TiO₂ 98 wt% and 2 wt% graphene; however, design 2 has the highest average response value, 1.0586, when compared to design 1 and 3, which have 1.0577 and 1.0339, respectively.

Table 4.3: Response value to ethanol gas

| Design | Paste | Response |
|--------|----------|----------|
| 1 | T99_G1_1 | 1.0698 |
| | T98_G2_1 | 1.0906 |
| | T95_G5_1 | 1.0126 |
| 2 | T99_G1_2 | 1.0616 |
| | T98_G2_2 | 1.0366 |
| | T95_G5_2 | 1.0777 |
| 3 | T99_G1_3 | 1.0073 |
| | T98_G2_3 | 1.0669 |
| | T95_G5_3 | 1.0276 |

CHAPTER 5

CONCLUSION AND FUTURE WORKS



5.1 Conclusion

In conclusion, this study offers a thorough examination of a manufactured gas sensor, emphasizing its construction, general overview, I-V characteristics, and performance assessment. Analyzing the I-V characteristics shows how the sensor behaves electrically in response to varying gas concentrations which is resistance values decrease as the concentration of graphene in the sensing material rises. The three constructed gas sensor designs are shown and each has distinct resistance values and I-V characteristics. The electrode and sensing material area in a gas sensor is a critical parameter that affects the contact resistance. With the three-design structure of TiO₂/graphene gas sensor, the expected I-V characteristics is in Schottky junction which resembles a diode but the result shows that all the structure produce linear graph

which resemble a resistor. Although the result is different, this TiO₂/graphene gas sensor manage to response to target gases.

The sensors are subjected to ethanol and acetone gasses as part of the performance evaluation process, which produces unique response patterns. Both target gases cause the gas sensor to react visibly and response values greater than 1 indicate sensitivity. Design 3 has higher response to acetone gas with the average value of 1.0255 compared to design 1 and 2 which has the average value of 1.0117 and 1.0222 respectively while design 2 has higher response to ethanol gas with the average value of 1.0586 compared to design 1 and 3 which has 1.0577 and 1.0339 respectively. The results open the door to possible improvements in sensor optimization and design, offering insightful information for the advancement of gas sensing technologies and real-world uses.

5.2 Future Works

Future studies on the TiO₂/graphene Schottky junction gas sensor project is optimizing the gas-sensitive layer's composition and thickness because it can lead to higher sensitivity and selectivity, which can improve the Schottky junction gas sensor's design structure. To get a Schottky diode characteristic, a new design structure is proposed for a better result. Figure 5.1 (a) shows the new design structure while (b) is the sensing material and (c) is the electrode.

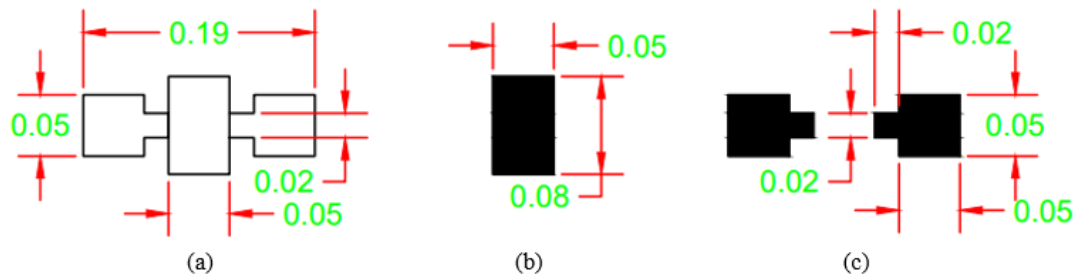


Figure 5.1: New design of Schottky junction structure (a) Layout of new structure of Schottky junction, (b) Sensing material layout, and (c) Electrode layout

Furthermore, incorporate advanced materials and nanostructures to augment the surface area can lead to improving response speed. Next, to increase its performance by adjusting the ratio of TiO_2 to graphene or by looking into using different materials such as SnO_2 due to its superior sensing performance to get more gas sensitivity. Production could become more reliable and scalable by improving manufacturing procedures and maximizing connection formation with various metals. Furthermore, the flexibility of the sensor in different situations may be enhanced by examining the impacts of temperature and applying real-time monitoring through IoT integration.

REFERENCES

- [1] D. Chen *et al.*, “High sensitive room temperature NO₂ gas sensor based on the avalanche breakdown induced by Schottky junction in TiO₂-Sn₃O₄ nanoheterojunctions,” *J Alloys Compd*, vol. 912, Aug. 2022, doi: 10.1016/j.jallcom.2022.165079.
- [2] B. Das, S. Behera, B. Satpati, and R. Ghosh, “Layered SnS₂/porous nickel foil based Schottky junction: An excellent ammonia sensor at room temperature,” *J Hazard Mater*, vol. 428, Apr. 2022, doi: 10.1016/j.jhazmat.2022.128252.
- [3] I. Jahangir, M. A. Uddin, A. Franken, A. K. Singh, and G. Koley, “Investigation of graphene/InN nanowire based mixed dimensional barristors with widely tunable Schottky barrier for highly sensitive multimodal gas sensing applications,” *Sens Actuators B Chem*, vol. 379, Mar. 2023, doi: 10.1016/j.snb.2022.133238.
- [4] Q. Pan, T. Li, and D. Zhang, “Ammonia gas sensing properties and density functional theory investigation of coral-like Au-SnSe₂ Schottky junction,” *Sens Actuators B Chem*, vol. 332, Apr. 2021, doi: 10.1016/j.snb.2021.129440.
- [5] I. P. Liu, C. H. Chang, B. Y. Ke, and K. W. Lin, “Study of a GaN Schottky diode based hydrogen sensor with a hydrogen peroxide oxidation approach and platinum catalytic metal,” *Int J Hydrogen Energy*, vol. 44, no. 60, pp. 32351–32361, Dec. 2019, doi: 10.1016/j.ijhydene.2019.10.112.

- [6] V. R. Naganaboina and S. G. Singh, "CdS based chemiresistor with Schottky contact: Toxic gases detection with enhanced sensitivity and selectivity at room temperature," *Sens Actuators B Chem*, vol. 357, Apr. 2022, doi: 10.1016/j.snb.2022.131421.
- [7] L. Guo, Z. Shen, C. Ma, C. Ma, J. Wang, and T. Yuan, "Gas sensor based on MOFs-derived Au-loaded SnO₂ nanosheets for enhanced acetone detection," *J Alloys Compd*, vol. 906, Jun. 2022, doi: 10.1016/j.jallcom.2022.164375.
- [8] S. Liu *et al.*, "ZnO/Ti₃C₂ composite with oxygen vacancies and Schottky barrier for effective detection of ppb-level NO₂ at room temperature," *Appl Surf Sci*, vol. 610, Feb. 2023, doi: 10.1016/j.apsusc.2022.155440.
- [9] D. L. Kong *et al.*, "Ag-nanoparticles-anchored mesoporous In₂O₃ nanowires for ultrahigh sensitive formaldehyde gas sensors," *Mater Sci Eng B Solid State Mater Adv Technol*, vol. 291, May 2023, doi: 10.1016/j.mseb.2023.116394.
- [10] L. Guo, H. Liang, D. An, and H. Yang, "One-step hydrothermal synthesis of uniform Ag-doped SnO₂ nanoparticles for highly sensitive ethanol sensing," *Physica E Low Dimens Syst Nanostruct*, vol. 151, Jul. 2023, doi: 10.1016/j.physe.2023.115717.
- [11] K. Xu, Z. Kan, F. Zhang, Y. Qu, S. Li, and S. Liu, "Hollow multi-shelled structural SnO₂ with multiple spatial confinement for ethanol gas sensing," *Mater Lett*, vol. 338, May 2023, doi: 10.1016/j.matlet.2023.134070.
- [12] S. Walke, M. B. Mandake, M. Naniwadekar, R. W. Tapre, T. Ghosh, and Y. Qureshi, "A review on copper chemical vapour deposition," *Mater Today Proc*, 2023, doi: 10.1016/j.matpr.2022.12.140.
- [13] H. Mousavi, Y. Mortazavi, A. A. Khodadadi, M. H. Saberi, and S. Alirezaei, "Enormous enhancement of Pt/SnO₂ sensors response and selectivity by their reduction, to CO in automotive exhaust gas pollutants including CO, NO_x and C₃H₈," *Appl Surf Sci*, vol. 546, Apr. 2021, doi: 10.1016/j.apsusc.2021.149120.
- [14] J. T. Mazumder *et al.*, "First principle study on structural and optoelectronic properties and band-gap modulation in germanium incorporated tin (IV) oxide," *Mater Today Commun*, vol. 27, Jun. 2021, doi: 10.1016/j.mtcomm.2021.102393.

- [15] P. M. Gadhavi, P. Poopanya, and M. Talati, "Structural, electronic, and transport properties of Ge doped graphene: A DFT study," *Physica B Condens Matter*, p. 415085, Oct. 2023, doi: 10.1016/j.physb.2023.415085.
- [16] K. Wu, W. Zhang, Z. Zheng, M. Debliquy, and C. Zhang, "Room-temperature gas sensors based on titanium dioxide quantum dots for highly sensitive and selective H₂S detection," *Appl Surf Sci*, vol. 585, May 2022, doi: 10.1016/j.apsusc.2022.152744.
- [17] Z. Ye *et al.*, "Excellent ammonia sensing performance of gas sensor based on graphene/titanium dioxide hybrid with improved morphology," *Appl Surf Sci*, vol. 419, pp. 84–90, Oct. 2017, doi: 10.1016/j.apsusc.2017.03.251.
- [18] C. Zarzeka *et al.*, "Use of titanium dioxide nanoparticles for cancer treatment: A comprehensive review and bibliometric analysis," *Biocatalysis and Agricultural Biotechnology*, vol. 50, Elsevier Ltd, Jul. 01, 2023. doi: 10.1016/j.bcab.2023.102710.
- [19] F. G. Aras *et al.*, "A review on recent advances of chemical vapor deposition technique for monolayer transition metal dichalcogenides (MX₂: Mo, W; S, Se, Te)," *Materials Science in Semiconductor Processing*, vol. 148, Elsevier Ltd, Sep. 01, 2022. doi: 10.1016/j.mssp.2022.106829.
- [20] K. Kamataki *et al.*, "Low-temperature fabrication of silicon nitride thin films from a SiH₄+N₂ gas mixture by controlling SiN_x nanoparticle growth in multi-hollow remote plasma chemical vapor deposition," *Mater Sci Semicond Process*, vol. 164, Sep. 2023, doi: 10.1016/j.mssp.2023.107613.
- [21] K. Tang, G. Wang, Q. Ruan, F. Peng, H. Cao, and P. K. Chu, "Controllable deposition of MoS₂ nanosheets on titanium by the vapor-phase hydrothermal technique and comparison with the conventional liquid-phase hydrothermal method," *Surf Coat Technol*, vol. 404, Dec. 2020, doi: 10.1016/j.surfcoat.2020.126497.
- [22] H. Krajian, B. Abdallah, M. Kakhia, and N. AlKafri, "Hydrothermal growth method for the deposition of ZnO films: Structural, chemical and optical studies," *Microelectronics Reliability*, vol. 125, Oct. 2021, doi: 10.1016/j.microrel.2021.114352.

- [23] G. Liang *et al.*, “Development of the screen-printed electrodes: A mini review on the application for pesticide detection,” *Environmental Technology and Innovation*, vol. 28. Elsevier B.V., Nov. 01, 2022. doi: 10.1016/j.eti.2022.102922.
- [24] M. Behera, R. Panda, P. Dhivya, D. Joshi, and R. Arun Kumar, “Study of efficient sustainable phosphor in glass (P – i – G) material for white LED applications fabricated by tape casting and screen-printing techniques,” *Materials Science and Engineering: B*, vol. 298, p. 116811, Dec. 2023, doi: 10.1016/j.mseb.2023.116811.
- [25] C. Zhou *et al.*, “Techniques for wearable gas sensors fabrication,” *Sensors and Actuators B: Chemical*, vol. 353. Elsevier B.V., Feb. 15, 2022. doi: 10.1016/j.snb.2021.131133.
- [26] G. Yeom, D. Kwon, W. Shin, M. K. Park, J. J. Kim, and J. H. Lee, “Fast-response/recovery In₂O₃ thin-film transistor-type NO₂ gas sensor with floating-gate at low temperature,” *Sens Actuators B Chem*, vol. 394, Nov. 2023, doi: 10.1016/j.snb.2023.134477.
- [27] T. Nakayama, Y. Kangawa, and K. Shiraishi, “Atomic Structures and Electronic Properties of Semiconductor Interfaces,” *Comprehensive Semiconductor Science and Technology*, vol. 1–6, pp. 113–174, Jan. 2011, doi: 10.1016/B978-0-44-453153-7.00052-3.
- [28] A. J. Ruys, “SiC Single Crystal Semiconductors,” *Silicon Carbide Ceramics*, pp. 165–214, Jan. 2023, doi: 10.1016/B978-0-323-89869-0.00004-6.
- [29] L. Schirone and P. Granello, “The power diode,” *Encyclopedia of Electrical and Electronic Power Engineering*, pp. 92–105, Jan. 2023, doi: 10.1016/B978-0-12-821204-2.00161-6.
- [30] T. Aernouts, W. Geens, J. Poortmans, J. Nijs, and R. Mertens, “Analysis and simulation of the IV-characteristics of PPV-oligomer based Schottky diodes.”

- [31] J. Ding *et al.*, “Recent progress in chemiresistive gas sensors with 1D nanostructured sensing materials: Insights into the structure-morphology-performance relationship,” *Mater Des*, vol. 234, Oct. 2023, doi: 10.1016/j.matdes.2023.112360.
- [32] S. Liu *et al.*, “Enhanced NO₂ gas-sensing performance of 2D Ti₃C₂/TiO₂ nanocomposites by in-situ formation of Schottky barrier,” *Appl Surf Sci*, vol. 567, Nov. 2021, doi: 10.1016/j.apsusc.2021.150747.
- [33] Y. Seekaew, A. Wisitsoraat, D. Phokharatkul, and C. Wongchoosuk, “Room temperature toluene gas sensor based on TiO₂ nanoparticles decorated 3D graphene-carbon nanotube nanostructures,” *Sens Actuators B Chem*, vol. 279, pp. 69–78, Jan. 2019, doi: 10.1016/j.snb.2018.09.095.
- [34] S. A. Mohd Chachuli, Y. Pei Yeuan, O. Coban, N. H. Shamsudin, and M. I. Idris, “Investigation of Graphene Gas Sensor at Different Substrates for Acetone Detection,” *Przegląd Elektrotechniczny*, vol. 99, no. 3, pp. 289–293, 2023, doi: 10.15199/48.2023.03.51.
- [35] S. A. M. Chachuli, M. L. H. Noor, O. Coban, N. H. Shamsudin, and M. I. Idris, “Characteristic of graphene-based thick film gas sensor for ethanol and acetone vapor detection at room temperature,” *Indonesian Journal of Electrical Engineering and Computer Science*, vol. 32, no. 3, pp. 1384–1391, 2023, doi: 10.11591/IJEECS.V32.I3.PP1384-1391.